ELSEVIER

Marine Chemistry 64 (1999) 199–227

MARINE CHEMISTRY

A diffusion-reaction model of carbon isotope fractionation in foraminifera

Richard E. Zeebe *, Jelle Bijma [1], Dieter A. Wolf-Gladrow [2]

Alfred-Wegener-Institut für Polar- und Meeresforschung, Postfach 12 01 61, D-27515, Bremerhaven, Germany

Received 17 September 1997; accepted 29 June 1998

Abstract

Fossil foraminiferal shells are utilized in paleoceanography to extract information about environmental conditions of the past ocean. Based on several assumptions, the ratio of ^{13}C and ^{12}C preserved in their shells is used to reconstruct, for example, the paleoproductivity or the oceanic pCO_2. Metabolism of the living organism and the sea water chemistry, however, can influence the incorporation of carbon isotopes during calcification such that the signal of the shells differ from the signal of the sea water. These effects occur because the chemical microenvironment of the foraminifer (boundary layer thickness ~ 500 μm) differs from the bulk sea water. Here, we present a numerical model that calculates the $\delta^{13}C$ of the foraminiferal shell as a function of the sea water chemistry and the magnitude of vital effects. Concentration profiles of the chemical species of the carbonate system within the microenvironment of foraminifera are obtained by solving diffusion-reaction equations. The compounds of dissolved forms of carbon dioxide containing either the stable carbon isotope ^{13}C or ^{12}C are considered separately. Spherical symmetry of the foraminifer is assumed. The model outcome is compared to results from culture experiments with the planktonic foraminifer *Orbulina universa*. Model results indicate that the interaction between vital effects of the foraminifer and the sea water chemistry can account for changes in the $\delta^{13}C$ of foraminiferal calcite of 0.3–0.4‰ when glacial and interglacial sea water conditions are compared. These effects occur even though the $\delta^{13}C$ of the total dissolved inorganic carbon is kept constant. Thus, changes in sea water chemistry should be distinguished from events which changed the $\delta^{13}C$ of the inorganic carbon of the sea water.

Keywords: foraminifera; paleoceanography; sea water; carbon isotopes

1. Introduction

The $\delta^{13}C$ of foraminiferal shells is routinely used as a proxy for $\delta^{13}C$ of the total dissolved inorganic carbon (ΣCO_2) of the sea water. This value can, for example, be employed to yield information about carbon fluxes between ocean and land biosphere on geological time scales (e.g., Shackleton et al., 1983). During the last

* Corresponding author. Tel.: +49-471-4831-812; Fax: +49-471-4831-425; E-mail: rzeebe@awi-bremerhaven.de

[1] Present address: Geosciences, University of Bremen, P.O. Box 330 440, D-28334 Bremen, Germany. E-mail: jbijma@uni-bremen.de.

[2] E-mail: wolf@awi-bremerhaven.de.

0304-4203/99/$ - see front matter
PII: S0304-4203(98)00075-9

decades it has become evident that foraminiferal calcite does not record the characteristics of the sea water by a simple 1:1 relationship. It was clearly demonstrated that the metabolism of the organism and the chemical state of the sea water affect the $\delta^{13}C$ of the calcite shells in the species *Orbulina universa*, *Globigerina bulloides* (Spero and Williams, 1988; Spero and Lea, 1996; Spero et al., 1997), *Globigerinoides sacculifer*, and *Globigerinoides ruber* (Bijma et al., unpublished data). These results demand an understanding of the mechanisms which influence the stable carbon isotope discrimination within the shells before experimentally determined relationships (e.g., $\delta^{13}C$ vs. $[CO_3^{2-}]$) can be extrapolated back into the past for the reconstruction of ocean history.

Foraminifera are unicellular marine organisms which build calcareous shells of diameters ranging approximately from 0.1 to 1 mm (for review of these and other calcareous species, see for example, Hemleben et al., 1989 and Wefer and Berger, 1991). Foraminifera are distributed throughout the entire world ocean, living in a benthonic or a planktonic habitat. A total of forty-four recent planktonic foraminiferal species are known, from which twenty-one species are common in the world's ocean. Planktonic foraminifera secrete a calcite test ($CaCO_3$) that includes a series of chambers coiled about an axis according to a planispiral or trochospiral mode. The geographic distribution of the different species is restricted to global climate belts and five major faunal provinces (polar, subpolar, transitional, subtropic, and tropic) were recognized (e.g., Bé, 1977). The distribution of species appears to be clearly related to water mass temperature but the factors governing abundance and range are certainly more complex. Foraminifera can be divided into non-spinose and spinose species. In general, the non-spinose species are herbivorous and most of the spinose species are carnivorous and harbor large numbers of actively photosynthesizing symbiotic algae between their spines (Hemleben et al., 1989).

The assumption inherent to all proxies is that they are mostly unequivocal and truly reflect the characteristics of the reconstructed parameter. For example, it is often presupposed that the isotopic signal of oxygen and carbon of the sea water is preserved in foraminiferal shells and is not affected by the living organism. However, life processes of the host-symbiont system such as respiration, photosynthesis of the symbiotic algae, and calcification can strongly influence the signal. These life processes are called vital effects (Spero and DeNiro, 1987; Spero and Williams, 1988). In addition, it was recently demonstrated for the planktonic foraminifera *O. universa* and *G. bulloides* that the isotopic composition of the calcite strongly depends on the carbonate chemistry of the sea water even if the isotopic composition of ΣCO_2 is not changed. A change of the seawater chemistry for the last glacial maximum (0.2–0.3 units increase in pH as proposed by Sanyal et al. (1995)) would produce a 0.3 to 0.4‰ decrease in the $\delta^{13}C$ of foraminiferal shells (Spero et al., 1997).

The differences between the signal of the bulk medium and the signal stored in the shells may be explained by an alteration of the isotopic composition of carbon at the site of calcification; i.e., the carbonate system and the $\delta^{13}C$ change markedly within the microenvironment of the foraminifer. To elucidate the nature of these processes, we have developed a numerical model of the carbonate system within the foraminiferal microenvironment that includes calculations of the concentrations of the stable carbon isotopes ^{13}C and ^{12}C. The goal of this paper is to provide a model that explains changes of the $\delta^{13}C$ of foraminiferal calcite attributed to changes of the sea water chemistry and vital effects which otherwise could be misinterpreted as changes of the $\delta^{13}C$ of the sea water.

2. Modelled species

As model species for carbon isotope fractionation in foraminiferal calcite the planktonic foraminifer *O. universa* was chosen (the applicability of our results to other species will be discussed in the concluding section). *O. universa* secretes a terminal spherical chamber which contains 90 to 100% of the total shell mass. This species is therefore ideal for culture experiments and for numerical modeling because the calcite of the terminal chamber is precipitated under controlled laboratory conditions. In addition, spherical geometry of the shell is an assumption for model purposes and is fulfilled by this species. Since numerous studies have been

carried out to examine the effect of light, temperature, and the sea water chemistry on the isotopic composition of the shell of *O. universa* (e.g., Spero and DeNiro, 1987; Spero and Williams, 1988; Spero et al., 1997) the model outcome can be directly compared to laboratory investigations.

O. universa has a tropical to temperate distribution and the salinity and temperature limits are 23–46 and 12°–31°C, respectively. Like most spinose species, *O. universa* is carnivorous and mainly feed on calanoid copepods at a rate of one to two per day. A large number of photosynthetic active symbiotic algae cells (up to ca. 7000) are harbored between the spines of *O. universa*. For a more detailed description of *O. universa* and associated life processes, see Wolf-Gladrow et al. (1999, this issue).

3. Model description

The model is based on the diffusion-reaction model in spherical geometry by Wolf-Gladrow et al. (1999, this issue) which describes the influence of vital effects on the inorganic carbonate system in the vicinity of foraminiferal shells. A brief recapitulation of this model will be given in Section 3.1, whereas Section 3.2 will focus on the inclusion of the different stable carbon isotopes to calculate the inorganic isotopic fractionation of the species of the carbonate system. Section 3.3 will describe the parameterization of the biological processes associated with the host-symbiont system such as respiration, photosynthesis, and calcification.

3.1. The existing diffusion-reaction model

The diffusion-reaction model by Wolf-Gladrow et al. (1999) calculates concentration profiles of chemical species of the carbonate system as a function of the distance to the center of the foraminiferal shell. The bulk sea water concentrations of CO_2, HCO_3^-, CO_3^{2-}, $B(OH)_3$, and $B(OH)_4^-$ depend on temperature, salinity, ΣCO_2, and the pH. Given the equilibrium values of the chemical reaction constants (DOE, 1994), the bulk concentrations can be calculated. The volume of the water surrounding the foraminifer is large compared to the size of the foraminifer, i.e., far away from the shell (~ 3000 μm) the concentration of all chemical substances will equal their bulk values (outer boundary condition). In the close vicinity of the foraminiferal shell, however, where CO_2 is released by respiration, carbon is taken up through photosynthesis, and calcite is precipitated, the concentrations of the chemical species differ from the bulk medium. A schematic representation of the model is given in Fig. 1.

The temporal change in the concentration $c(r,t)$ of a species of the carbonate system at distance r to the center of the shell is determined by diffusion, chemical reaction and uptake or release of this species. At steady state, the fluxes are in equilibrium and $\partial c/\partial t$ is zero. Thus, the model equations are of the form:

$$0 = \frac{\partial c(r,t)}{\partial t} = \text{Diffusion} + \text{Reaction} + \text{Uptake}$$

3.1.1. Diffusion

The diffusion term in spherical coordinates reads:

$$\text{Diffusion} = \frac{D_c}{r^2}\frac{\mathrm{d}}{\mathrm{d}r}\left(r^2\frac{\mathrm{d}c}{\mathrm{d}r}\right)$$

where D_c is the diffusion coefficient of the chemical species c. Diffusion coefficients at a specific temperature were taken from Jähne et al. (1987) for CO_2, from Li and Gregory (1974) for HCO_3^-, CO_3^{2-}, H^+, and OH^-, from Mackin (1986) for $B(OH)_3$, and from Boudreau and Canfield (1993) for $B(OH)_4^-$. The temperature and salinity dependence of the diffusion coefficients were taken into account by the Stokes–Einstein relation (e.g., Cussler, 1984).

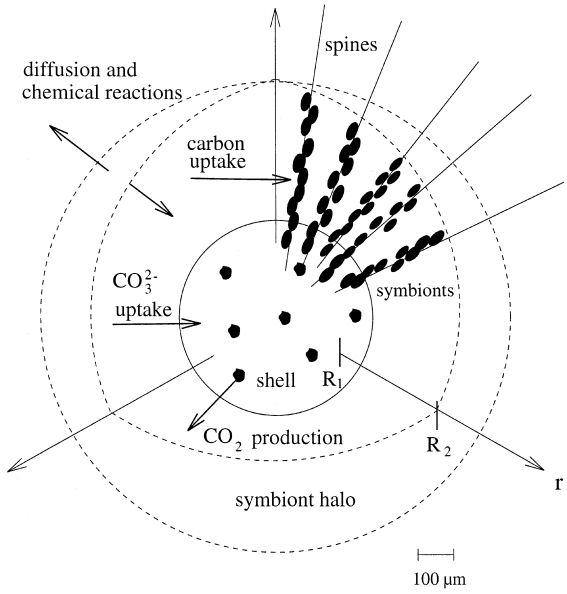

Fig. 1. Schematic illustration of the spherical model of the foraminifer. The foraminiferal shell is approximated by a sphere (R_1). Respired CO_2 diffuses through apertures of the shell. Calcification is modelled by the uptake of CO_3^{2-} and Ca^{2+} at the surface of the shell. The photosynthesizing symbiotic algae are attached to the spines of the foraminifer and are located within a halo around the shell (R_2). Model equations describe diffusion and chemical conversion of dissolved carbon compounds including the stable carbon isotopes ^{13}C and ^{12}C.

3.1.2. Chemical reactions

The chemical reactions between carbon species, water, and borate considered in the model are (in this paper the notation $CO_2 \equiv CO_2(aq.)$ is used):

$$CO_2 + H_2O \underset{k_{-1}}{\overset{k_{+1}}{\rightleftharpoons}} H^+ + HCO_3^- \tag{1}$$

$$CO_2 + OH^- \underset{k_{-4}}{\overset{k_{+4}}{\rightleftharpoons}} HCO_3^- \tag{2}$$

$$CO_3^{2-} + H^+ \underset{k_{-5}}{\overset{k_{+5}}{\rightleftharpoons}} HCO_3^- \tag{3}$$

$$H_2O \underset{k_{-6}}{\overset{k_{+6}}{\rightleftharpoons}} H^+ + OH^- \tag{4}$$

$$B(OH)_3 + H_2O \underset{k_{-7}}{\overset{k_{+7}}{\rightleftharpoons}} B(OH)_4^- + H^+ \tag{5}$$

where k_+ and k_- are reaction rates of the forward and backward reaction, respectively. In the literature, k_2 and k_3 are often used for reactions including carbonic acid (H_2CO_3) and are therefore omitted here. Carbonic acid which always occurs in negligible concentrations is taken into account by the effective reaction (1). For details and values of the reaction rates, see Wolf-Gladrow and Riebesell (1997). Equilibrium constants K are related to the reaction rates by $K = k_+/k_-$. Numerical values for equilibrium constants (depending on sea water

temperature and salinity) were taken from DOE (1994). Fig. 2 displays the concentrations of the dissolved carbon species CO_2, HCO_3^-, and CO_3^{2-} in equilibrium as a function of pH. The concentrations of CO_2 and CO_3^{2-} exhibit large changes in the pH range from 7 to 9. While the concentration of CO_2 decreases from about 200 to 1 μmol kg^{-1}, the concentration of CO_3^{2-} increases from about 10 to over 800 μmol kg^{-1} (note the logarithmic scale of the vertical axis). Even though, HCO_3^- changes by ca. 800 μmol kg^{-1} within the considered pH range the relative change in the concentration of HCO_3^- is small compared to the relative variations in the concentrations of CO_2 and CO_3^{2-}.

3.1.3. Uptake

Uptake of species of the carbonate system is either specified as source/sink-term in the model equations or as a boundary condition. The volume described by the model is a shell of a sphere extending from the surface of the foraminiferal shell (inner boundary, $r = R_1$) to the bulk sea water (outer boundary, $R_3 = 10 \times R_1$). Calcification was implemented in the model by the uptake of CO_3^{2-} and Ca^{2+} ions at the inner boundary, i.e., the inner boundary condition for CO_3^{2-} is given by the calcification flux at the surface of the shell. Photosynthesis and respiration of the symbiotic algae occur within a halo surrounding the shell, resulting in a sink and source term in the equations for CO_2 and HCO_3^- (the neutrality of ion fluxes into the cell during HCO_3^- uptake is modelled by a simultaneous H^+ uptake or the release of OH^- ions, for further discussion, see Wolf-Gladrow et al. (1999)). Respiration of the foraminifer represents the inner boundary condition for CO_2.

3.1.4. Diffusion-reaction equations

As an example, the diffusion-reaction equation for CO_2 is considered:

$$0 = \frac{D_{CO_2}}{r^2}\frac{\mathrm{d}}{\mathrm{d}r}\left(r^2\frac{\mathrm{d}[CO_2]}{\mathrm{d}r}\right) + \left(k_{-1}[H^+] + k_{-4}\right)[HCO_3^-] - \left(k_{+1} + k_{+4}[OH^-]\right)[CO_2] + f_{res}^{CO_2} - f_{phs}^{CO_2} \quad (6)$$

where D_{CO_2} is the diffusion coefficient of CO_2, r is the distance to the center of the foraminiferal shell, and k's are reaction constants (Wolf-Gladrow and Riebesell, 1997). The source and sink of CO_2 through respiration and photosynthesis of the symbiotic algae, is denoted by $f_{res}^{CO_2}$ and $f_{phs}^{CO_2}$, respectively. The complete set of equations for total carbon compounds ($C = {}^{13}C + {}^{12}C$) for the various components of the carbonate system is given in Wolf-Gladrow et al. (1999).

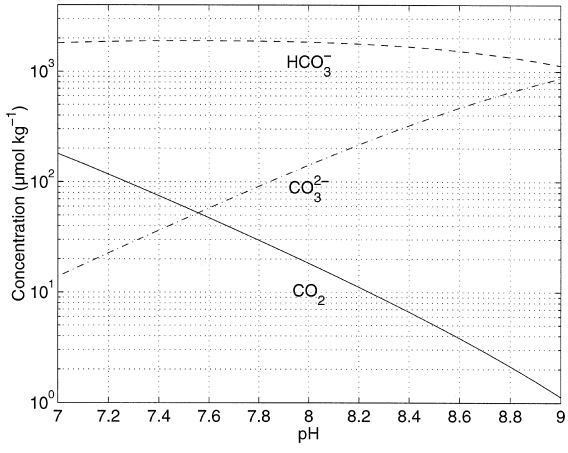

Fig. 2. Concentrations of the dissolved carbon species as a function of pH. While the concentration of CO_2 decreases dramatically within the considered pH range, the concentration of CO_3^{2-} increases.

3.2. Equations for ^{13}C isotopes

Model Eqs. such as (6) describe the reaction, diffusion and uptake of the components of the carbonate system. The concentration of each carbon species, i.e., $[CO_2]$, $[HCO_3^-]$, or $[CO_3^{2-}]$, represents the concentration of the sum of the stable carbon isotopes ^{13}C and ^{12}C within this species. We found that solving equations for ^{13}C and for the sum of ^{13}C and ^{12}C was equivalent to the concept of solving equations for ^{13}C and for ^{12}C when the mathematics were done thoroughly. In this paper, the former approach was chosen.

$$\left[CO_2\right] = \left[^{12}CO_2\right] + \left[^{13}CO_2\right]$$

$$\left[HCO_3^-\right] = \left[H^{12}CO_3^-\right] + \left[H^{13}CO_3^-\right]$$

$$\left[CO_3^{2-}\right] = \left[^{12}CO_3^{2-}\right] + \left[^{13}CO_3^{2-}\right]$$

To determine the isotopic ratio of the carbon species within the microenvironment of the foraminifer three more equations for $^{13}CO_2$, $H^{13}CO_3^-$, and $^{13}CO_3^{2-}$ are included. Once, the concentration profiles of the ^{13}C species have been found, the isotopic ratio ($^{13}C/^{12}C$) and thus the $\delta^{13}C$ values of the carbon species can be calculated.

The chemical reactions including ^{13}C are:

$$^{13}CO_2 + H_2O \underset{k'_{-1}}{\overset{k'_{+1}}{\rightleftharpoons}} H^+ + H^{13}CO_3^- \tag{7}$$

$$^{13}CO_2 + OH^- \underset{k'_{-4}}{\overset{k'_{+4}}{\rightleftharpoons}} H^{13}CO_3^- \tag{8}$$

$$^{13}CO_3^{2-} + H^+ \underset{k'_{-5}}{\overset{k'_{+5}}{\rightleftharpoons}} H^{13}CO_3^- \tag{9}$$

where the k' are the reaction rates for the chemical reactions associated with ^{13}C compounds. Therefore, the diffusion-reaction equations for the ^{13}C components read

$^{13}CO_2$:

$$0 = \frac{D_{^{13}CO_2}}{r^2}\frac{\mathrm{d}}{\mathrm{d}r}\left(r^2\frac{\mathrm{d}\left[^{13}CO_2\right]}{\mathrm{d}r}\right) + \left(k'_{-1}[H^+] + k'_{-4}\right)\left[H^{13}CO_3^-\right] - \left(k'_{+1} + k'_{+4}[OH^-]\right)\left[^{13}CO_2\right] + {}^{13}f_{\mathrm{res}}^{CO_2} - {}^{13}f_{\mathrm{phs}}^{CO_2} \tag{10}$$

$H^{13}CO_3^-$:

$$0 = \frac{D_{H^{13}CO_3}}{r^2}\frac{\mathrm{d}}{\mathrm{d}r}\left(r^2\frac{\mathrm{d}\left[H^{13}CO_3^-\right]}{\mathrm{d}r}\right) + k'_{+1}\left[^{13}CO_2\right] - k'_{-1}[H^+]\left[H^{13}CO_3^-\right] - k'_{-4}\left[H^{13}CO_3^-\right] + k'_{+4}\left[^{13}CO_2\right][OH^-] - k'_{-5}\left[H^{13}CO_3^-\right] + k'_{+5}[H^+]\left[^{13}CO_3^{2-}\right] - {}^{13}f_{\mathrm{phs}}^{HCO_3^-} \tag{11}$$

$^{13}CO_3^{2-}$:

$$0 = \frac{D_{^{13}CO_3}}{r^2}\frac{\mathrm{d}}{\mathrm{d}r}\left(r^2\frac{\mathrm{d}\left[^{13}CO_3^{2-}\right]}{\mathrm{d}r}\right) + k'_{-5}\left[H^{13}CO_3^-\right] - k'_{+5}[H^+]\left[^{13}CO_3^{2-}\right] \tag{12}$$

The diffusion-reaction equations for H^+ and OH^- do not need to be modified because the ^{13}C compounds (which react with H^+ and OH^-) are already included in the total concentration of the carbon species. The diffusion coefficient for $^{13}CO_2$ was taken from O'Leary (1984) ($D_{^{12}CO_2}/D_{^{13}CO_2} = 1.0007$), while for HCO_3^- and CO_3^{2-} the diffusion coefficients of the ^{13}C and ^{12}C species were assumed to be equal. The HCO_3^- and CO_3^{2-} ions are surrounded by a significant number of water molecules of hydration which contribute to the effective size of the molecule. Thus, the effect of the ^{13}C atom on the effective size of the molecule and thus on the diffusion coefficient is probably very small (O'Leary, pers. comm. 1996).

The chemical equilibrium constants of the corresponding reactions of the ^{13}C species are:

$$K_1' = \frac{[H^+]\left[H^{13}CO_3^-\right]}{\left[^{13}CO_2\right]} \tag{13}$$

$$\frac{K_1'}{K_w} = \frac{\left[H^{13}CO_3^-\right]}{\left[^{13}CO_2\right][OH^-]} \tag{14}$$

$$K_2' = \frac{\left[^{13}CO_3^{2-}\right][H^+]}{\left[H^{13}CO_3^-\right]} \tag{15}$$

where K_1' and K_2' correspond to the first and second dissociation constant of carbonic acid; K_w is the ion product of water. The reaction rates k' and equilibrium constants K' for the ^{13}C species are not the same as for ^{12}C. Their values must be inferred from measurements of the isotopic composition of the carbon species.

3.2.1. Equilibrium constants

The differences between the equilibrium constants of the chemical reactions of the ^{13}C and ^{12}C species lead to fractionation effects between the different carbon species. In equilibrium CO_2 is about 9‰ 'lighter' than HCO_3^- (i.e., the $\delta^{13}C$ of CO_2 is more negative), while CO_3^{2-} is about 0.5‰ 'lighter' than HCO_3^- at 25°C. To comprehend the mathematics involved in the following calculations it is useful to recapitulate the definitions of R, α, ε, and δ values. For example, the isotopic ratio R of CO_2 is defined as:

$$R_{CO_2} = \frac{\left[^{13}CO_2\right]}{\left[^{12}CO_2\right]}$$

whereas the fractionation factor between CO_2 and HCO_3^- is defined by $\alpha_{(CO_2-HCO_3^-)}$:

$$\alpha_{(CO_2-HCO_3^-)} = \frac{R_{CO_2}}{R_{HCO_3^-}}$$

Since α values are generally very close to 1.0, ε values are used to express the isotopic ratio in per mill:

$$\varepsilon_{(CO_2-HCO_3^-)} = \left(\alpha_{(CO_2-HCO_3^-)} - 1\right) \times 1000.$$

The $\delta^{13}C$ is used to compare isotopic compositions with a standard ratio. For example, the $\delta^{13}C$ of CO_2 is defined as

$$\delta^{13}C_{CO_2} = \left(\frac{R_{CO_2}}{R_{PDB}} - 1\right) \times 1000$$

where $R_{PDB} = 0.01124$ is the standard ratio ($^{13}C/^{12}C$) of the fossil belemnite from the Pee Dee Formation in South Carolina (O'Leary, 1981). The fractionation factors ε for carbonate species and calcite were taken from Mook (1986):

$$\varepsilon_1 := \varepsilon_{(CO_2(g)-HCO_3^-)} = -9483/T + 23.89 \quad (16)$$

$$\varepsilon_2 := \varepsilon_{(CO_2-CO_2(g))} = -373/T + 0.19 \quad (17)$$

$$\varepsilon_3 := \varepsilon_{(CO_2-HCO_3^-)} = -9866/T + 24.12 \quad (18)$$

$$\varepsilon_4 := \varepsilon_{(CO_3^{2-}-HCO_3^-)} = -867/T + 2.52 \quad (19)$$

$$\varepsilon_5 := \varepsilon_{(CaCO_3(calc)-HCO_3^-)} = -4232/T + 15.10 \quad (20)$$

$$\varepsilon_6 := \varepsilon_{(CaCO_3(calc)-CO_3^{2-})} = -3341/T + 12.54 \quad (21)$$

where T is the absolute temperature in Kelvin. Eq. (21) was calculated from Eqs. (19) and (20).

Using Eqs. (18) and (19), and the definition of ε values, isotopic ratios α for the dissolved forms of carbon dioxide can be calculated.

$$\alpha_3 := \frac{\left[^{13}CO_2\right]/\left[^{12}CO_2\right]}{\left[H^{13}CO_3^-\right]/\left[H^{12}CO_3^-\right]} = \varepsilon_3 \times 10^{-3} + 1 \quad (22)$$

$$\alpha_4 := \frac{\left[^{13}CO_3^{2-}\right]/\left[^{12}CO_3^{2-}\right]}{\left[H^{13}CO_3^-\right]/\left[H^{12}CO_3^-\right]} = \varepsilon_4 \times 10^{-3} + 1 \quad (23)$$

Isotopic ratios for the chemical reactions of the total carbon compounds (1)-(5) and the ^{13}C compounds (7)-(9) are given by the ratio of the equilibrium constants:

$$K_1/K_1' = \left(\frac{\left[^{13}CO_2\right]/[CO_2]}{\left[H^{13}CO_3^-\right]/[HCO_3^-]} \right)_1 \quad (24)$$

$$K_2'/K_2 = \left(\frac{\left[^{13}CO_3^{2-}\right]/[CO_3^{2-}]}{\left[H^{13}CO_3^-\right]/[HCO_3^-]} \right)_2 \quad (25)$$

The conversion between CO_2 and HCO_3^- occurs mainly via reaction (7) at low pH and via reaction (8) at high pH. However, the isotopic ratio of CO_2 and HCO_3^- in equilibrium does not depend on the reaction way between the both species (thermodynamic constraint). Thus, the isotopic ratio of CO_2 and HCO_3^- in equilibrium is given by Eq. (24). The chemical equilibrium constants K_1' and K_2' for the reactions of the ^{13}C compounds can therefore be calculated from the fractionation factors given by Mook and the isotopic ratios Eqs. (24) and (25).

$$K_1' = K_1/\alpha_3' \quad (26)$$

$$K_2' = K_2 \times \alpha_4' \quad (27)$$

where factors α' slightly differ from α because the fractionation factors α are given for the ratio $[^{13}C]/[^{12}C]$ while K/K' reflects the ratio of $[^{13}C]/([^{13}C]+[^{12}C])$. For example, α_4' is given by:

$$\alpha_4' = \alpha_4 \frac{1 - \left[^{13}CO_3^{2-}\right]/\left[CO_3^{2-}\right]}{1 - \left[H^{13}CO_3^-\right]/[HCO_3^-]}$$

The error using α instead of α' expressed in terms of $\delta^{13}C$ would be in the order of 0.1‰. Thus, α' (exact value) was used in the model calculations since even small changes are important when discussing for e.g., the $\delta^{13}C$ of the total dissolved carbon of the ocean.

3.2.2. Reaction rates

Equilibrium fractionation is a result of the kinetic fractionation of the forward and backward chemical reaction. For example, the hydration step of CO_2 to HCO_3^- (reaction (1) forward) results in a lighter HCO_3^- of about 13‰. On the other hand, the dehydration step (reaction (1) backward) results in a lighter CO_2 of about 22‰ (O'Leary et al., 1992). The difference between the forward and backward reaction equals the equilibrium fractionation between CO_2 and HCO_3^- of about 9‰ (the equilibrium value given by Mook (1986) is 8.97‰ at 25°C). Generally, the relationship between equilibrium fractionation (K/K') and kinetic fractionation ($k_{\pm}/k'_{\pm}$) can be written as

$$\frac{K}{K'} = \alpha = \frac{k_+ \times k'_-}{k_- \times k'_+} \tag{28}$$

where α is the equilibrium fractionation factor of the corresponding chemical reaction. Values for the ratios of reaction rates for the hydration and hydroxylation of CO_2 (Eqs. (1) and (2) forward) implemented in the model are

$$k'_{+1}/k_{+1} = 0.987 \quad \text{at } 24°C, \quad \text{O'Leary et al., 1992} \tag{29}$$

$$k'_{+4}/k_{+4} = 0.989 \quad \text{O'Leary (pers. comm.)} \tag{30}$$

The temperature dependence of the kinetic fractionation was taken into account by the temperature dependence of the equilibrium fractionation (α is a function of the temperature, compare e.g., Eqs. (18) and (22)). Values for the dehydration and dehydroxylation (Eqs. (1) and (2) backward) were calculated from equilibrium fractionation:

$$k'_{-1}/k_{-1} = 0.987 \times \alpha_3 \tag{31}$$

$$k'_{-4}/k_{-4} = 0.989 \times \alpha_3 \tag{32}$$

The fact that there are no data available for k'_{+5}, and k'_{-5} is of minor importance because the equilibrium fractionation between HCO_3^- and CO_3^{2-} is very small (~ 0.5‰). It is much smaller than the fractionation between CO_2 and HCO_3^- because the proton transfer reaction is several orders of magnitude faster than the carbon–oxygen bond change reaction. The values of k'_{+5} and k'_{-5} were set consistently with Eq. (28). The effect on the model outcome was negligible when k'_{+5}/k_{+5} and k'_{-5}/k_{-5} were varied between 1 and 0.999, which is twice the equilibrium fractionation.

3.2.3. Initializing $\delta^{13}C$ values

In addition to the initialization of the bulk concentrations of the carbon species [$^{13}C + {}^{12}C$], which is done by using chemical equilibrium constants, the bulk concentrations of the ^{13}C carbon species (and thus the bulk $\delta^{13}C$ values) have to be initialized. This is done by using the $\delta^{13}C$ value of the total dissolved CO_2 which is an input parameter to the model.

The $\delta^{13}C$ value of the total dissolved CO_2 is defined as:

$$\delta^{13}C_{\Sigma CO_2} := \left(\delta^{13}C_{CO_2}[CO_2] + \delta^{13}C_{HCO_3^-}[HCO_3^-] + \delta^{13}C_{CO_3^{2-}}\left[CO_3^{2-}\right]\right)/[\Sigma CO_2]$$

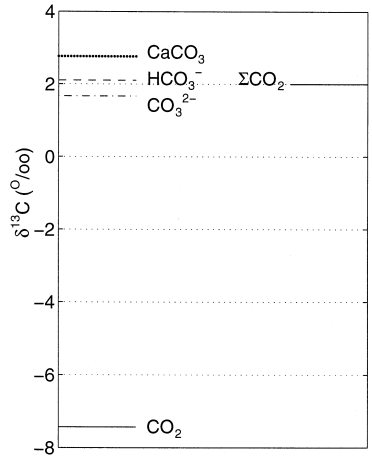

Fig. 3. Fractionation between the species of the carbonate system at pH 8.15 and a temperature of 20°C. Values for equilibrium fractionation are taken from Mook (1986). The $\delta^{13}C$ of ΣCO_2 is 2‰. Variations in pH from 7.5 to 9 have little effect on the isotopic compositions of the carbon species (< 0.2‰). The large fractionation effect between HCO_3^- and CO_2 results from the break of the carbon–oxygen bond during chemical conversion.

with

$$\delta^{13}C_{CO_2} = \left(\frac{R_{CO_2}}{R_{PDB}} - 1 \right) \times 1000$$

$$\delta^{13}C_{HCO_3^-} = \left(\frac{R_{HCO_3^-}}{R_{PDB}} - 1 \right) \times 1000$$

$$\delta^{13}C_{CO_3^{2-}} = \left(\frac{R_{CO_3^{2-}}}{R_{PDB}} - 1 \right) \times 1000$$

Using fractionation factors Eqs. (18) and (19), and neglecting terms $\varepsilon \times 10^{-3}$, the bulk $\delta^{13}C$ values of the carbon species can be determined: [3]

$$\delta^{13}C_{HCO_3^-} = \delta^{13}C_{\Sigma CO_2} - \frac{\varepsilon_3[CO_2] + \varepsilon_4[CO_3^{2-}]}{[\Sigma CO_2]} \tag{33}$$

$$\delta^{13}C_{CO_2} = \delta^{13}C_{HCO_3^-} + \varepsilon_3 \tag{34}$$

$$\delta^{13}C_{CO_3^{2-}} = \delta^{13}C_{HCO_3^-} + \varepsilon_4 \tag{35}$$

Fig. 3 displays the $\delta^{13}C$ of the different carbon species and of $CaCO_3$ at a temperature of 20°C and a $\delta^{13}C_{\Sigma CO_2}$ of 2‰ at pH = 8.15. The $\delta^{13}C$ of the carbon species change less than 0.2‰ within the pH range from 7.5 to 9. This range covers the pH changes in the ambient environment of a foraminifer as well as changes of sea water conditions during culture experiments. The $\delta^{13}C$ of HCO_3^- and CO_3^{2-} are similar because the addition or release of H^+ has little effect on the isotopic fractionation. The $\delta^{13}C$ of CO_2 is, however, about 9‰ more negative than the $\delta^{13}C$ of CO_3^{2-}. This effect can be explained by the break-up of the carbon–oxygen bond which leads to a higher fractionation than the proton transfer in the case of HCO_3^- and CO_3^{2-}.

[3] In the numerical model the exact formula was used (including terms $\varepsilon \times 10^{-3}$ which are omitted here for simplicity).

3.3. Mathematical description of biological processes

In the previous sections, the abiotic part (chemical reactions, inorganic isotope fractionation, etc.) of the model was described. Vital effects of the living organism such as respiration, photosynthesis of the symbiotic dinoflagellates, and calcification are also included in the model calculations. The mathematical description of these biological processes are presented in this section. Total fluxes of the life processes are denoted by an uppercase F (e.g., F_{res}) whereas a lowercase f refers to the uptake or release of a chemical species at distance r to the center of the foraminiferal shell (e.g., $f_{\mathrm{phs}}^{\mathrm{CO}_2}(r)$).

3.3.1. Respiration

Respiration of the foraminifer and of the symbiotic algae produce CO_2 which is depleted in ^{13}C. Isotopic analyses of *Artemia* used as food source in culture experiments with *O. universa* gave a $\delta^{13}C$ value of $-21.9‰$ (Spero, 1992). It was assumed that the respired CO_2 exhibits the same isotopic composition as the food source and the $\delta^{13}C$ of the respiration flux F_{res} was therefore set at $-21.9‰$. The ^{13}C flux was determined from the definition of the $\delta^{13}C$ values:

$$\delta^{13}\mathrm{C}_{F,\mathrm{res}} = \left(\frac{{}^{13}F_{\mathrm{res}} / {}^{12}F_{\mathrm{res}}}{R_{\mathrm{PDB}}} - 1 \right) \times 1000 \tag{36}$$

and the total flux F_{res}:

$$F_{\mathrm{res}} = {}^{12}F_{\mathrm{res}} + {}^{13}F_{\mathrm{res}} \tag{37}$$

Combination of Eqs. (36) and (37) yields:

$${}^{13}F_{\mathrm{res}} = F_{\mathrm{res}} \frac{1}{1 + \left[R_{\mathrm{PDB}} \left(\delta^{13}\mathrm{C}_{F,\mathrm{res}} \times 10^{-3} + 1 \right) \right]^{-1}} \tag{38}$$

3.3.2. Photosynthesis

Photosynthesis of the microalgae preferentially consumes $^{12}CO_2$ and possibly $H^{12}CO_3^-$, resulting in an enrichment of ^{13}C within the microenvironment of the foraminifer. The uptake of CO_2 ($^{12}CO_2 + {}^{13}CO_2$) by photosynthesis is described by Michaelis–Menten kinetics, while the HCO_3^- uptake is calculated as the difference between the total carbon uptake and the CO_2 uptake (for detail see Wolf-Gladrow et al. (1999)). The $\delta^{13}C$ of the photosynthetic product therefore depends on the ratio of the CO_2 and HCO_3^- flux because the carbon sources exhibit different $\delta^{13}C$ values. In this section an expression will be derived for the ^{13}C fluxes of CO_2 and HCO_3^- during photosynthesis. Once, these fluxes have been determined, the enrichment of ^{13}C in the microenvironment of the foraminifer can be calculated. This enrichment is eventually reflected in the calcite.

From the definition of the $\delta^{13}C$ (example CO_2):

$$\delta^{13}\mathrm{C}_{\mathrm{phs}}^{\mathrm{CO}_2}(r) = \left(\frac{{}^{13}f_{\mathrm{phs}}^{\mathrm{CO}_2}(r) / {}^{12}f_{\mathrm{phs}}^{\mathrm{CO}_2}(r)}{R_{\mathrm{PDB}}} - 1 \right) \times 1000$$

and the fluxes at r:

$$f_{\mathrm{phs}}^{\mathrm{CO}_2}(r) = {}^{12}f_{\mathrm{phs}}^{\mathrm{CO}_2}(r) + {}^{13}f_{\mathrm{phs}}^{\mathrm{CO}_2}(r)$$

one obtains:

$$^{13}f_{\mathrm{phs}}^{\mathrm{CO_2}}(r) = f_{\mathrm{phs}}^{\mathrm{CO_2}}(r)\,\frac{1}{1+\left[R_{\mathrm{PDB}}\left(\delta^{13}\mathrm{C}_{\mathrm{phs}}^{\mathrm{CO_2}}(r)\times 10^{-3}+1\right)\right]^{-1}} \tag{39}$$

$$^{13}f_{\mathrm{phs}}^{\mathrm{HCO_3^-}}(r) = f_{\mathrm{phs}}^{\mathrm{HCO_3^-}}(r)\,\frac{1}{1+\left[R_{\mathrm{PDB}}\left(\delta^{13}\mathrm{C}_{\mathrm{phs}}^{\mathrm{HCO_3^-}}(r)\times 10^{-3}+1\right)\right]^{-1}} \tag{40}$$

where $f_{\mathrm{phs}}^{\mathrm{CO_2}}(r)$ and $f_{\mathrm{phs}}^{\mathrm{HCO_3^-}}(r)$ are the fluxes of $^{12}CO_2 + {}^{13}CO_2$ and $H^{12}CO_3^- + H^{13}CO_3^-$ through photosynthesis associated with the respective $\delta^{13}C$ of these fluxes, namely $\delta^{13}\mathrm{C}_{\mathrm{phs}}^{\mathrm{CO_2}}(r)$ and $\delta^{13}\mathrm{C}_{\mathrm{phs}}^{\mathrm{HCO_3^-}}(r)$. Since these fluxes have already been calculated by the model via Michaelis–Menten kinetics, the remaining unknown variable is the $\delta^{13}C$ of the CO_2 and HCO_3^- flux, respectively. The $\delta^{13}C$ of the CO_2 and HCO_3^- uptake of the symbionts is calculated as:

$$\delta^{13}\mathrm{C}_{\mathrm{phs}}^{\mathrm{CO_2}}(r) = \delta^{13}\mathrm{C}_{\mathrm{CO_2}}(r) - \varepsilon_{\mathrm{p}}^{\mathrm{CO_2}} \tag{41}$$

$$\delta^{13}\mathrm{C}_{\mathrm{phs}}^{\mathrm{HCO_3^-}}(r) = \delta^{13}\mathrm{C}_{\mathrm{HCO_3^-}}(r) - \varepsilon_{\mathrm{p}}^{\mathrm{HCO_3^-}} \tag{42}$$

where $\varepsilon_{\mathrm{p}^{\mathrm{CO_2}}}$ and $\varepsilon_{\mathrm{p}}^{\mathrm{HCO_3^-}}$ is the fractionation factor for CO_2 and HCO_3^- uptake, respectively. The literature reports values for the fractionation in marine dinoflagellates between 18‰ to 29.7‰ (Descolas-Gros and Fontugne, 1985; Wong and Sackett, 1978; Falkowski, 1991), referring to an overall $\bar{\varepsilon}_{\mathrm{p}} := \delta^{13}\mathrm{C}_{\Sigma\mathrm{CO_2}} - \delta^{13}\mathrm{C}_{\mathrm{POM}}$. In order to cover the range of the reported fractionation values, the fractionation factors $\varepsilon_{\mathrm{p}}^{\mathrm{CO_2}}$ and $\varepsilon_{\mathrm{p}}^{\mathrm{HCO_3^-}}$ were set to a value of 18‰ and are therefore assumed to be identical for CO_2 and HCO_3^- uptake: If HCO_3^- was the exclusive source for photosynthesis the $\delta^{13}C$ of organic matter would be about -18‰ ($\delta^{13}\mathrm{C}_{\mathrm{POM}} = \delta^{13}\mathrm{HCO_3^-} - \varepsilon_{\mathrm{p}}^{\mathrm{HCO_3^-}} \approx 0-18 = -18$). If CO_2 was the exclusive source for photosynthesis the $\delta^{13}C$ of organic matter would be about -27‰ ($\delta^{13}\mathrm{C}_{\mathrm{POM}} = \delta^{13}\mathrm{C}_{\mathrm{CO_2}} - \varepsilon_{\mathrm{p}}^{\mathrm{CO_2}} \approx -9-18 = -27$).

The fractionation of carbon isotopes during carbon assimilation by phytoplankton is a complex process and subject of intensive investigations (e.g., Rau et al., 1992; Francois et al., 1993; Goericke and Fry, 1994; Rau et al., 1996). These studies demonstrate that the ^{13}C fractionation may vary with temperature, the carbon dioxide concentration of the bulk medium, nutrients, and light. For example, a common observed feature is that $\bar{\varepsilon}_{\mathrm{p}}$ is decreasing with decreasing CO_2 concentration. This effect is included in Eqs. (41) and (42) because the total carbon uptake of the symbionts is divided into CO_2 uptake (described by Michaelis–Menten kinetics) and HCO_3^- uptake (calculated as the difference between total carbon demand and CO_2 uptake). The overall fractionation ($\bar{\varepsilon}_{\mathrm{p}}$) is therefore decreasing with decreasing CO_2 concentration because more carbon in the form of HCO_3^- is taken up which is isotopically heavier than the carbon dioxide.

Unfortunately, no data are available on the response of the ^{13}C fractionation in the symbiotic dinoflagellates to variations of other parameters such as temperature, nutrients, and light. Hence, constant $\varepsilon_{\mathrm{p}}^{\mathrm{CO_2}}$ and $\varepsilon_{\mathrm{p}}^{\mathrm{HCO_3^-}}$ were chosen in the model to avoid further complications at this stage and because the fractionation of carbon isotopes during symbiont photosynthesis is one of the many aspects of the entire concept.

3.3.3. Calcification

The goal of the model is to calculate the $\delta^{13}C$ of the shell to understand the interaction of vital effects and the sea water chemistry which affect the isotopic composition of the calcite. The model results will be used to investigate to which extent the life processes mask the $\delta^{13}C$ of ΣCO_2 that the shell $\delta^{13}C$ is thought to have. In the previous sections, it was described how respiration and photosynthesis are implemented in the model and thereby affect the isotopic composition of CO_2 and HCO_3^- in the vicinity of the foraminifer. Part of the isotopically altered carbon diffuses away from the shell, part of it is chemically converted and eventually incorporated into the shell.

Chamber calcification in foraminifera commences at a so called primary organic membrane on which calcite is precipitated (e.g., Hemleben et al., 1989). Laboratory observations indicate that CO_3^{2-} is probably the

primary source for calcification because shell weight increases with increasing carbonate ion concentration (Bijma et al., in press). If not stated otherwise, calcification in the model is described by the uptake of CO_3^{2-} and Ca^{2+} at the inner boundary $r = R_1$, where R_1 is the radius of the shell (the effect of HCO_3^- utilization is discussed in Section 4.3.1). The process thus consumes CO_3^{2-} from a reservoir with a certain $^{13}C/^{12}C$ ratio given by $[^{13}CO_3^{2-}]_{R_1}/[^{12}CO_3^{2-}]_{R_1}$. In addition, the calcification reaction discriminates against the light isotope; $CaCO_3$ is 1‰ 'heavier' than CO_3^{2-} ((Romanek et al., 1992), see Fig. 3). Thus, the ratio of the calcification fluxes can be written as

$$\frac{^{13}F_{clc}}{^{12}F_{clc}} = \alpha_6 \frac{\left[^{13}CO_3^{2-}\right]_{R_1}}{\left[^{12}CO_3^{2-}\right]_{R_1}}. \tag{43}$$

where $\alpha_6 = \alpha_{(CaCO_3(calc)-CO_3^{2-})}$ is the discrimination factor between CO_3^{2-} and $CaCO_3$. Eq. (43) indicates that $^{13}F_{clc}$ is itself a function of the solution of the model equations because the right hand side is calculated by numerical iteration. Thus, the calculated concentration profiles of $[^{13}CO_3^{2-}]$ and $[^{12}CO_3^{2-}]$, and $^{13}F_{clc}$ must satisfy the inner boundary condition (43). Once $^{13}F_{clc}$ has been calculated, the $\delta^{13}C$ of the shell is eventually given by:

$$\delta^{13}C_{sh} = \left(\frac{^{13}F_{clc}/^{12}F_{clc}}{R_{PDB}} - 1 \right) \times 1000 \tag{44}$$

4. Model results

In this section, we will investigate the influence of vital effects as well as the interaction between vital effects and the sea water chemistry on the model output (i.e., the $\delta^{13}C$ of the foraminiferal calcite). First, a qualitative introduction will be given in which the influence of respiration, calcification, and symbiont-photosynthesis is described. Subsequently, the model results for a combination of vital effects (dark and light experiments) and the model output including sea water chemistry changes will be discussed in detail. Eventually, model results are compared to laboratory data for *O. universa*. Based on this comparison it can be tested if the model adequately describes fractionation effects in *O. universa* and therefore furthers our understanding of the underlying mechanisms.

4.1. Vital effects

The influence of vital effects such as respiration, calcification, and photosynthesis on the carbonate system in the vicinity of the foraminifer was described by Wolf-Gladrow et al. (1999). To investigate the associated fractionation effects, we will now discuss the qualitative response of the shell $\delta^{13}C$ to the isotopically altered carbonate environment which is produced by vital effects.

4.1.1. Qualitative consideration

Respiration of the symbiotic algae and the foraminifer produce CO_2 which is depleted in ^{13}C. When inorganic carbon is fixed by the enzyme Rubisco (ribulose biphosphate carboxylase oxygenase) during photosynthesis it is associated with a large isotope fractionation of about -29‰ (O'Leary et al., 1992). The produced organic matter consequently exhibits a negative $\delta^{13}C$ value, i.e., it is isotopically 'light'. The isotopic composition of the respired CO_2 of the symbiotic algae reflects the $\delta^{13}C$ of the carbon during uptake and is therefore depleted in ^{13}C. Similarly, respired CO_2 of the foraminifer stems from organic matter (preferential food source are copepods) and is also 'light'. In summary, the microenvironment is enriched in 'light' carbon by respiration. Photosynthesis of the symbiotic algae, on the other hand, preferentially utilizes ^{12}C over ^{13}C

which results in an enrichment of ^{13}C in the microenvironment of the foraminifer. The environment is becoming isotopically 'heavy'.

Respiration (ca. 1–3 nmol h^{-1}) and photosynthesis (ca. 3–10 nmol h^{-1}) fluxes of carbon are associated with strong isotopic signals ($\delta^{13}C \sim -22‰$). The extent to which the microenvironment is isotopically altered therefore depends on the magnitude of the respiration/photosynthesis flux and on the $\delta^{13}C$ of the released and fixed carbon, respectively.

Calcite precipitation in equilibrium is accompanied by a small fractionation of 1‰ (Romanek et al., 1992) and is independent of the flux (ca. 1–3 nmol h^{-1}). Calcification therefore results in a direct enrichment of ^{13}C within the shell (there is no additional chemical conversion between the source of calcification (CO_3^{2-}) and the precipitated calcite ($CaCO_3$) as in the case of respired CO_2 and the CO_3^{2-} pool).

A schematic presentation of the influence of respiration, symbiont photosynthesis, and calcification on the $\delta^{13}C$ of the foraminiferal shell is provided by Fig. 4a. Starting with a $\delta^{13}C$ of the total dissolved carbon of 2‰,

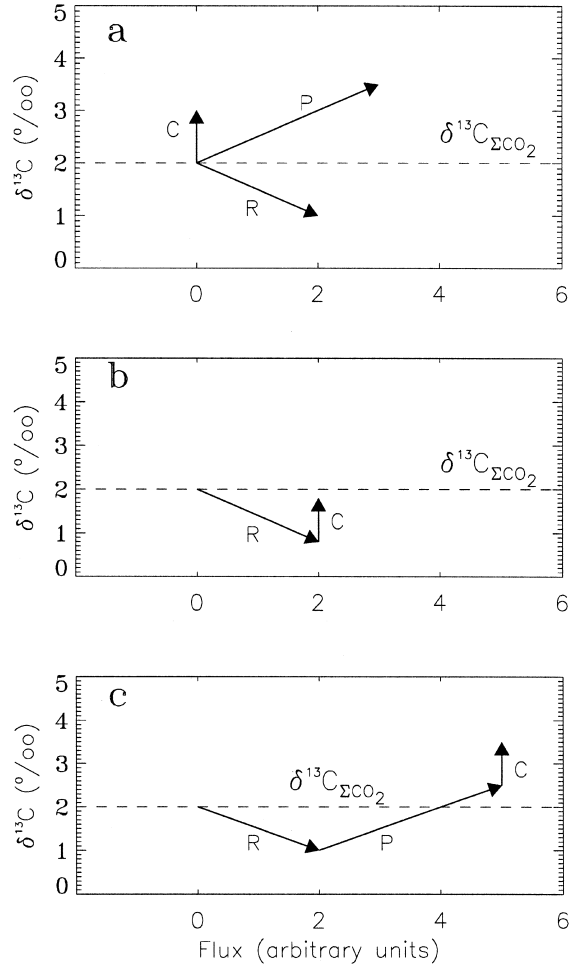

Fig. 4. Qualitative description of the influence of vital effects on the $\delta^{13}C$ of foraminiferal calcite. Adding up the vectors yields the $\delta^{13}C$ of the shell. (a) Respiration (R) and photosynthesis (P) decrease and increase the $\delta^{13}C$, respectively. Calcification (C) fractionates with a constant value, independent of the calcification rate. (b) Dark conditions: calcification effect may cancel respiration effect. (c) Light conditions: photosynthesis enriches the shell in ^{13}C. It should be noticed that the length and direction of the vectors may vary significantly for different foraminiferal species.

vectors are added to determine the final $\delta^{13}C$ of the shell ($\delta^{13}C_{sh}$). The obtained $\delta^{13}C_{sh}$ should be regarded as a qualitative result which cannot be generalized. The horizontal axis represents the flux, while the vertical axis refers to the $\delta^{13}C$ of the shell. The enrichment and depletion of ^{13}C in the shell through photosynthesis (P) and respiration (R) is a function of the magnitude of the associated flux. Photosynthesis is therefore presented by a vector with positive slope whereas respiration is presented by a vector with negative slope. For simplicity, a linear relationship between respiration/photosynthesis flux and $\delta^{13}C_{sh}$ is assumed. Calcification is described by a vertical vector of length 1‰ since the fractionation associated with calcification is independent of the flux. Even though, this description is highly simplified it illustrates the basic influence of the vital effects on the isotopic composition of the calcite and may help to understand the results of the detailed model.

For example, calcite precipitation during the night, when no photosynthesis occurs (Fig. 4b) can be described as follows. Starting with $\delta^{13}C_{\Sigma CO_2} = 2‰$, respiration (R) which produces isotopically 'light' carbon may decrease the $\delta^{13}C_{sh}$ to about 1‰. The fractionation during $CaCO_3$ precipitation (C), however, results in an increase in $\delta^{13}C_{sh}$ of ca. 1‰ and may bring the isotopic composition of the shell close to the δ value of ΣCO_2. We should emphasize here, that the length and direction of the vectors might vary significantly for different foraminiferal species. In the light, photosynthesis (P) of the symbiotic algae enriches the microenvironment in ^{13}C which is incorporated in the shell (Fig. 4c). The contribution of photosynthesis is added to respiration and calcification, ending up, for example at a $\delta^{13}C_{sh}$ which is 1 to 1.5‰ higher than the $\delta^{13}C$ of ΣCO_2. This qualitative description will be quantified in the next section where the model calculated contributions of the vital effects to the isotopic composition of the shell are discussed.

4.1.2. Results of the base model

Model results for light and dark experiments are studied for a set of input parameters (Table 1) corresponding to a model run for the planktonic foraminifer *O. universa*. Sea water salinity and temperature of the model calculations are similar to those reported for laboratory experiments (specimens for culture experiments were collected near Santa Catalina Island, California (33°33′N, 118°30′W) (e.g., Spero and DeNiro, 1987; Spero, 1992)).

Fig. 5 shows model results of a dark simulation for the $\delta^{13}C$ of the three dissolved carbon species and ΣCO_2 as a function of the distance to the center of the foraminiferal shell at $r = 0$. Towards the surface of the shell at $r = 300$ μm the $\delta^{13}C$ of CO_2 is strongly decreasing (Fig. 5a) due to the isotopically 'light' CO_2 which is

Table 1
Input variables for the base model run for *O. universa*

Variable	Symbol	Value	
Sea water temperature	T	20.0°C	
Sea water salinity	S	33.5	
Sea water pH	pH	8.15	
Sea water alkalinity	A_T	2400 μeq kg^{-1}	
Radius of shell	R_1	300 μm	
$\delta^{13}C$ of ΣCO_2	$\delta^{13}C_{\Sigma CO_2}$	2.0‰	
$\delta^{13}C$ of respiration	$\delta^{13}C_{F,res}$	−21.9‰[a]	
$\delta^{13}C$ of photosynthesis	$\delta^{13}C_{F,phs}$	see text	
		Dark	Light
Respiration flux	F_{res}	2.1	2.1 nmol h^{-1}[b]
Photosynthesis flux	F_{phs}	0.0	7.2 nmol h^{-1}[b]
Calcification flux	F_{clc}	1.0	3.0 nmol h^{-1}[c]

[a] Spero (1992).
[b] Spero et al. (1991).
[c] Lea et al. (1995).

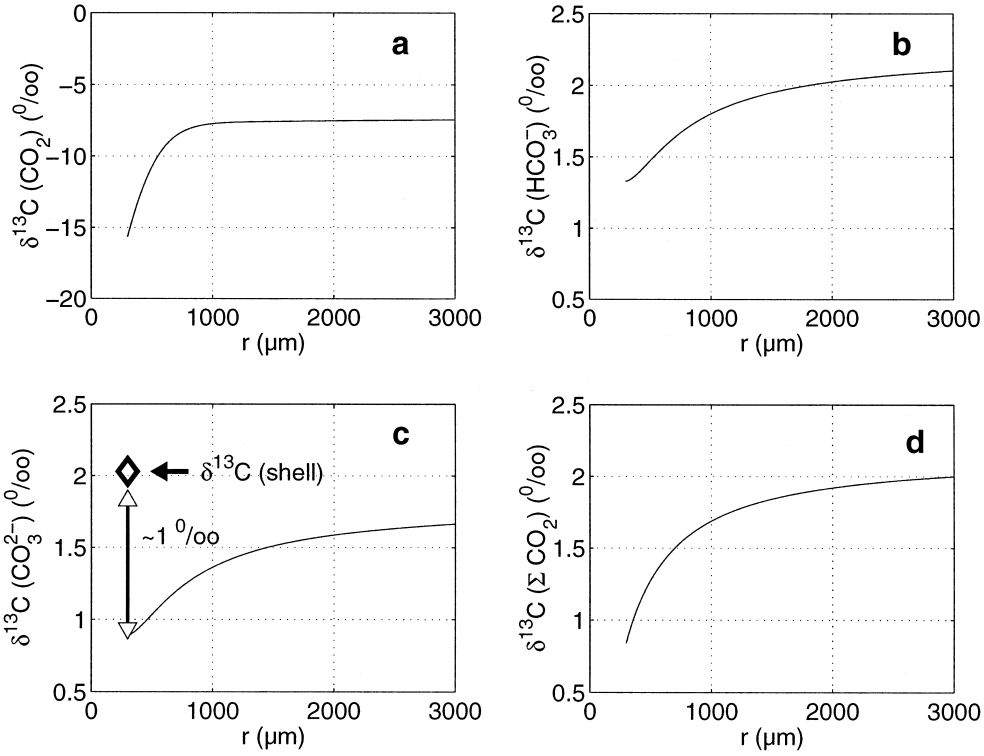

Fig. 5. Results of the base model in the dark for the $\delta^{13}C$ of (a) CO_2, (b) HCO_3^-, (c) CO_3^{2-}, and (d) ΣCO_2 as a function of the distance to the center of the shell r. Respired isotopically 'light' CO_2 decreases the $\delta^{13}C$ of CO_2 and consequently of CO_3^{2-} at the shell, while calcite precipitation increases $\delta^{13}C_{sh}$ by $\sim 1‰$. The final $\delta^{13}C$ of the shell is indicated by the diamond in (c).

released by respiration at this site. Part of the CO_2 is diffusing away from the shell, part of it is chemically converted to HCO_3^-, resulting in a decrease of the $\delta^{13}C$ of HCO_3^- at the shell (Fig. 5b). The signature of the respired CO_2 is strongly reflected in the CO_2 adjacent to the shell because this pool is small (ca. 13.4 μmol kg^{-1} in the bulk medium at pH 8.15, see Fig. 2). In other words, the proportion of respired CO_2 is large in comparison to the CO_2 close to the shell. The response in the $\delta^{13}C$ of HCO_3^- is much smaller because the chemical conversion is relatively slow and the HCO_3^- pool is much larger (ca. 2000 μmol kg^{-1}).

Since the reaction between HCO_3^- and CO_3^{2-} is fast, the isotopic exchange is fast, and the $\delta^{13}C$ signal in HCO_3^- is almost directly reflected in the $\delta^{13}C$ of CO_3^{2-} (Fig. 5c). In the model, calcification utilizes CO_3^{2-} for calcite precipitation. The calcite is enriched in ^{13}C relative to CO_3^{2-} (see Fig. 3). Consequently, the $\delta^{13}C$ of the shell (indicated by the diamond in Fig. 5c) is about 1.1‰ 'heavier' than the CO_3^{2-} and about 1.2‰ 'heavier' than the ΣCO_2 at the site of calcification, respectively. The enrichment of $CaCO_3$ of about 1‰ relative to CO_3^{2-} (Romanek et al., 1992) increases the $\delta^{13}C$ of the shell to about 1.9‰. Thus, the effect of respiration nearly cancels the effect of calcification for the base model run, resulting in a $\delta^{13}C$ of the shell which is close to $\delta^{13}C_{\Sigma CO_2}$ of the bulk medium.

Results of the base model for light conditions are shown in Fig. 6. Photosynthesis of the symbiotic algae (7.2 nmol C h^{-1}) which are located between 300 and 800 μm preferentially utilizes ^{12}C. The simultaneous enrichment of the environment in ^{13}C produces a maximum in $\delta^{13}C_{CO_2}$ within the symbiont halo at about 600 μm (Fig. 6a). At the surface of the shell respiration of the foraminifer dominates; the $\delta^{13}C$ of CO_2 decreases to about −15‰. The isotopic composition of HCO_3^- (Fig. 6b), however, demonstrates that photosynthesis is the major process influencing the $\delta^{13}C$ of HCO_3^- and consequently that of CO_3^{2-}; the $\delta^{13}C$ is increasing towards the

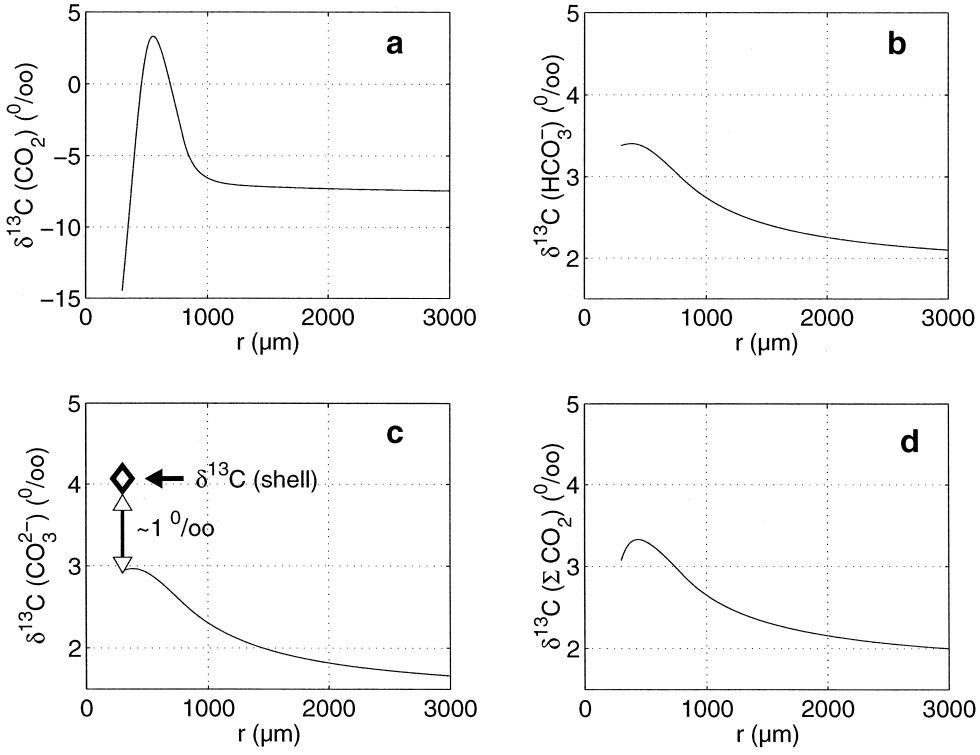

Fig. 6. Results of the base model in the light for the $\delta^{13}C$ of (a) CO_2, (b) HCO_3^-, (c) CO_3^{2-}, and (d) ΣCO_2 as a function of the distance to the center of the shell r. Photosynthesis of the symbiotic algae preferentially take up isotopically 'light' carbon. The simultaneous enrichment of the environment in 'heavy' carbon increases $\delta^{13}C_{sh}$. The final $\delta^{13}C$ of the shell is indicated by the diamond in (c). This value was calculated for a continuous photosynthetic rate of 7.2 nmol C h^{-1} (no day/night cycle).

shell. The release of 'light' CO_2 through respiration (2.1 nmol h^{-1}) cannot compensate the enrichment of 'heavy' CO_2 and HCO_3^- through photosynthesis (7.2 nmol h^{-1}). The model calculated $\delta^{13}C$ of the shell (indicated by the diamond in Fig. 6c) for the light experiment is 4.2‰. To obtain an estimate for the $\delta^{13}C$ of the shell for a natural day/night cycle, a mean value of $3.1‰ = (2.0‰ + 4.2‰)/2$ between dark and light conditions can be calculated.

4.1.3. Comparison with laboratory data: different light conditions

Extensive culture experiments with *O. universa* have been carried out to study the $\delta^{13}C$ and $\delta^{18}O$ of the calcite as a function of the light intensity (e.g., Spero and Williams, 1988; Spero, 1992). The laboratory data are used to test the model results for the dark and light experiment. Since culture data for the $\delta^{13}C$ of foraminiferal calcite are reported as a function of the light intensity in μEin m^{-2} s^{-1}, the photosynthetic rate in nmol mol h^{-1} (model input) has to be related to the light intensity. This is done by a formula for the P/I curve given by Jassby and Platt (1976):

$$F_{phs} = F_{phs}^{max} \tanh(I/I_k)$$

where F_{phs}^{max} is the maximum photosynthetic rate at light saturation, and $I_k = 100$ μEin m^{-2} s^{-1} is the light saturation intensity (Rink et al., 1998). (Rink measured photosynthetic rates in *O. universa* from which light saturation intensities were deduced. The measurements by oxygen microelectrodes yielded a mean value of ca. 100 μEin m^{-2} s^{-1} which was adapted for model purposes.)

Model results for the $\delta^{13}C$ of the shell as a function of the light intensity (lines) and laboratory data (circles) are shown in Fig. 7. Laboratory data are taken from Spero and Williams (1988); the $\delta^{13}C$ of the culture water was approximately 1.5‰. In the dark (light intensity zero) measured $\delta^{13}C$ of *Orbulina universa* are slightly higher than the $\delta^{13}C_{\Sigma CO_2}$ of the culture water which is in agreement with model results. At light saturation (Irradiance > 100 μEin m^{-2} s^{-1}) the measured values approach a value of ca. 3‰. The model results (solid and dashed lines) confirm the increase of $\delta^{13}C$ with increasing light intensity. The calculated curve for a medium photosynthetic rate of 7.2 nmol C h^{-1} (solid line) results in a predicted $\delta^{13}C$ of the calcite which is about 0.5‰ 'lighter' than observed values at light saturation. The calculated curve for the higher photosynthetic rate of 10.3 nmol C h^{-1} (dashed line) is in good agreement with the observed isotopic composition of the shells. The photosynthetic rates were taken from Spero et al. (1991) where the net assimilation rate of 7.2 and 10.3 nmol C h^{-1} corresponds to a density of 4200 and 6000 symbionts per foraminifera, respectively.

The increase of the $\delta^{13}C$ values in the 0–100 μEin m^{-2} s^{-1} range is a direct consequence of the shape of the P/I curve in the same range and therefore depends on the I_k value. To investigate the model outcome for different P/I curves the shell $\delta^{13}C$ values were calculated as a function of the light intensity for $I_k = 75$ and 100 μEin m^{-2} s^{-1} (smallest and mean value of *O. universa* given by Rink et al., 1998), and 170 μEin m^{-2} s^{-1} (determined for *G. sacculifer* by Jørgensen et al. (1985)). The results are shown in Fig. 8. Obviously, I_k values of 75–100 μEin m^{-2} s^{-1} given by Rink et al. (1998) are consistent with the laboratory data, whereas the larger value of 170 μEin m^{-2} s^{-1} does not produce a sufficient increase of the shell $\delta^{13}C$ at low light.

The saturation value of $\delta^{13}C$ at high light is, on the other hand, independent of the shape of the P/I curve. The saturation value is a function of the maximum photosynthetic rate which depends on symbiont density. Within the uncertainties of the biological input parameters the model adequately describes the increase of shell $\delta^{13}C$ vs. irradiance at low light and the saturation value of $\delta^{13}C$ at high light.

4.2. Carbonate sea water chemistry

The concentrations of the dissolved forms of CO_2, alkalinity, ΣCO_2, and pH of the bulk sea water are the variables of the carbonate sea water chemistry. The quantities are not independent of each other; given two of the quantities (and the borate concentration), all other components can be determined. In the previous sections, the influence of vital effects on the $\delta^{13}C$ of foraminiferal calcite was studied for a constant carbonate sea water chemistry representative for todays ocean (pH ≈ 8.15, alkalinity ≈ 2400 μEq kg^{-1}). On geological time scales, however, ocean chemistry may have changed markedly. For example, there is evidence that the pH of the

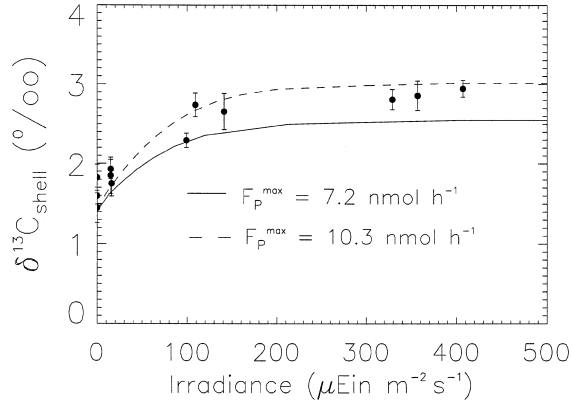

Fig. 7. Model results (lines) and laboratory data (closed circles) for the $\delta^{13}C$ of the calcite as a function of the light intensity. The maximum photosynthetic rate at light saturation of 7.2 (solid line) and 10.3 nmol C h^{-1} (dashed line) were taken from (Spero et al., 1991), corresponding to a maximum density of 4200 and 6000 symbionts per foraminifera, respectively.

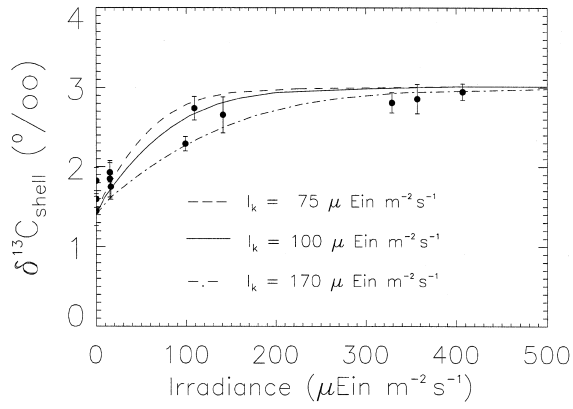

Fig. 8. Same as Fig. 7 with a maximum photosynthetic rate at light saturation of 10.3 nmol C h^{-1} and different I_k values. The curve of shell $\delta^{13}C$ vs. light intensity is a direct result of the P/I curve. Thus, a smaller I_k value (steeper increase of photosynthesis at low light) produces a steeper increase of $\delta^{13}C$. The saturation value of the shell $\delta^{13}C$ at the maximum photosynthetic rate is independent of the I_k value.

surface and the deep ocean during the last glaciation has been 0.2 and 0.3 units higher than today (Sanyal et al., 1995; Sanyal et al., 1996).

Spero et al. (1997) have shown, that the $\delta^{13}C$ of *O. universa* and *G. bulloides* strongly depend on the carbonate chemistry, even though the $\delta^{13}C$ of the total dissolved carbon in sea water is not affected by changes in the sea water chemistry. We suggest that these effects can be explained by an interaction between vital effects and the carbonate sea water chemistry of the bulk medium. To elucidate the nature of the underlying mechanisms the model was run for different conditions of the bulk carbonate system. Possible scenarios for pH changes were examined by setting the alkalinity to a constant value, while pH was varied over a considerable range. This approach provides a comparison with culture data of *O. universa*.

4.2.1. Constant alkalinity

To investigate the influence of varying bulk concentrations of CO_2, HCO_3^-, and CO_3^{2-} on the isotopic environment of the foraminiferal shell the dark experiment (see Section 4.1.2) is examined for different pH. The alkalinity is held constant at 2723 μeq kg^{-1} while pH is set at 7.7, 8.15, and 8.8; all other parameters are the same as for the base model run (see Table 1).

To understand the fractionation of carbon isotopes, the total concentrations of the dissolved carbon species are studied first. Model results for the concentrations of CO_2, HCO_3^-, CO_3^{2-}, and pH for the dark experiment are displayed in Fig. 9. The bulk concentration of CO_2 ($r = 3000$ μm) dramatically varies with pH (Fig. 9a). At pH 7.7 and pH 8.8, the concentration of CO_2 of the bulk medium is 2 and 50 μmol kg^{-1}, respectively. The steep increase of CO_2 towards the shell results from the respiration of the foraminifer. It should be emphasized that the concentration of CO_2 at the shell is about twice the bulk value at low pH (7.7) while it is about 10 times the bulk value at high pH (8.8).

No drastic change in the concentration profile of HCO_3^- was calculated (Fig. 9b) because bicarbonate is the largest pool and changes slowly over the considered pH range. The bulk concentration of CO_3^{2-}, however, strongly increases from 100 μmol kg^{-1} at pH 7.7 to over 600 μmol kg^{-1} at pH 8.8 (Fig. 9c). The decrease of CO_3^{2-} at the shell is due to the uptake of CO_3^{2-} for calcite precipitation (1 nmol h^{-1}). If CO_3^{2-} is the major source to form calcite, calcification is limited at low pH (7.7) by the small concentration of CO_3^{2-} at the shell. Culture experiments support this hypothesis because the foraminiferal shell weight of *O. universa* decreases with decreasing CO_3^{2-} concentration (Bijma et al., in press). In addition, calcification was incomplete or shells even dissolved over night when pH was below 7.3 (Bijma et al., unpublished data).

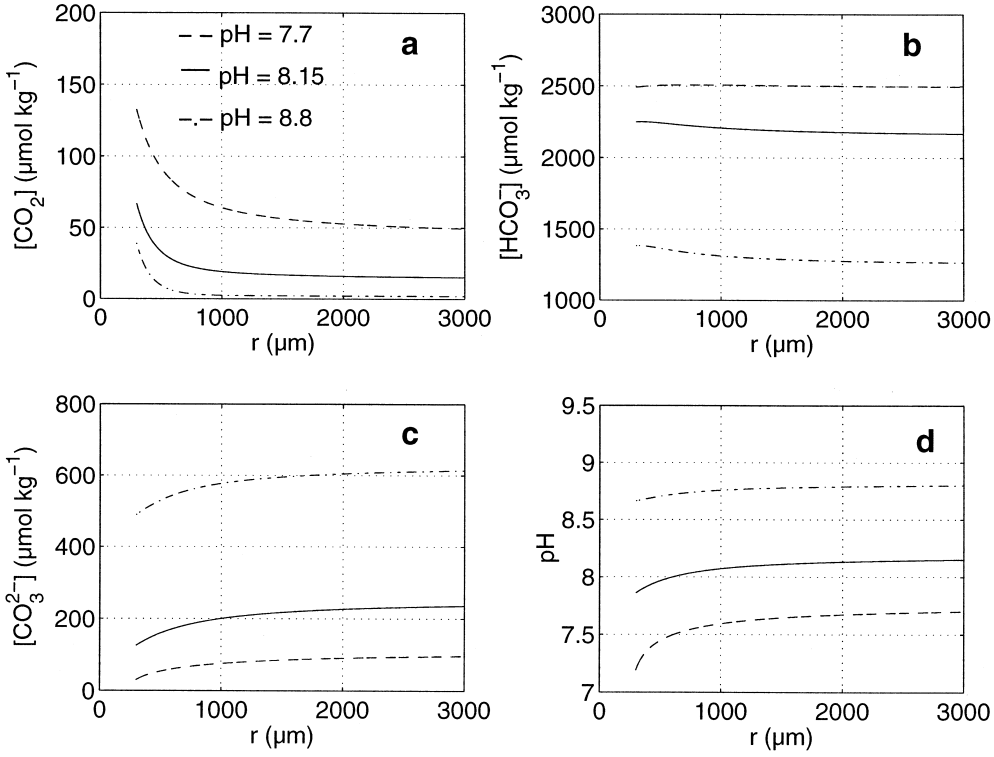

Fig. 9. Model results for the concentration profiles of (a) CO_2, (b) HCO_3^-, (c) CO_3^{2-}, and (d) pH in the dark for constant alkalinity (2723.0 μeq kg^{-1}). Results for different pH values of the bulk medium are indicated by dashed lines (pH 7.7), solid lines (pH 8.15), and dot–dashed lines (pH 8.8). Bulk concentrations of CO_2 and CO_3^{2-} vary dramatically with pH.

Fig. 10 shows model results of the corresponding profiles of $\delta^{13}C$. At the shell ($r = 300$ μm) the $\delta^{13}C$ of CO_2 is decreasing for the indicated bulk pH values. Isotopically 'light' carbon is released by the foraminifer and diffuses away from the shell (Fig. 10a). The decrease is most pronounced at high pH because the amount of respired CO_2 relative to the bulk concentration is extremely high (the concentration of CO_2 at the shell is 10 times higher than in the bulk medium). The 'light' CO_2 is partially converted to HCO_3^- resulting in a decrease of $\delta^{13}C$ of the bicarbonate and carbonate at the shell (Fig. 10b and c). Again, the lowest $\delta^{13}C$ of HCO_3^- and CO_3^{2-} at the shell was calculated for the highest pH. This trend is eventually reflected in the $\delta^{13}C$ of the shell (diamonds in Fig. 10c). In summary, the calculated $\delta^{13}C$ of the foraminiferal calcite in the dark is decreasing with increasing pH at constant alkalinity.

4.2.2. Comparison with laboratory data (dark conditions)

For the planktonic foraminifera *O. universa* culture experiments have demonstrated that the $\delta^{13}C$ values of the shell calcite decrease with increasing CO_3^{2-} ion concentration or pH (Spero et al., 1997). The model was run for the reported sea water conditions of the culture experiments of *O. universa* and a calcification/respiration rate of 1.0 and 2.1 nmol h^{-1}, respectively (see Table 1). Model results for the $\delta^{13}C$ of the shell under dark conditions (open diamonds) and laboratory data obtained in the dark (filled circles) are presented in Fig. 11. The expected $\delta^{13}C$ of inorganic calcite formed in equilibrium with the isotopic composition of the total dissolved carbon of the bulk sea water (calculated after Mook (1986)) is indicated by the dashed line. It is obvious that the $\delta^{13}C$ of the calcite precipitated within the microenvironment of *O. universa* differs significantly from the expected $\delta^{13}C$ of the calcite precipitated in equilibrium with $\delta^{13}C_{\Sigma CO_2}$.

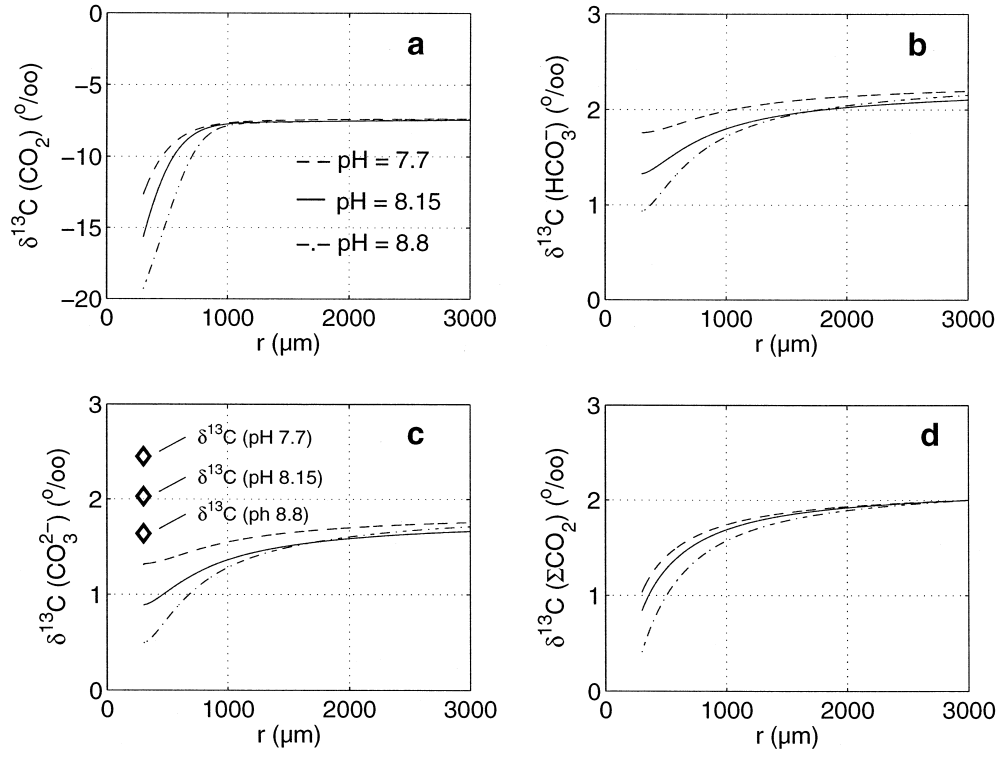

Fig. 10. Model results for the $\delta^{13}C$ of (a) CO_2, (b) HCO_3^-, (c) CO_3^{2-}, and (d) ΣCO_2 of the dark experiment corresponding to sea water conditions presented in Fig. 9. The diamonds in (c) indicate the $\delta^{13}C$ of the foraminiferal shell. Shell $\delta^{13}C$ decreases with increasing pH (CO_3^{2-} concentration).

Laboratory data show a large scatter even for small changes in $[CO_3^{2-}]$, while the model results exhibit a continuous decrease with increasing pH. The model calculated $\delta^{13}C$ values centered around 200 μmol kg^{-1} must be regarded as an exception. The alkalinity of the culture water was exceptionally low ($\sim$ 2160 μeq kg^{-1})

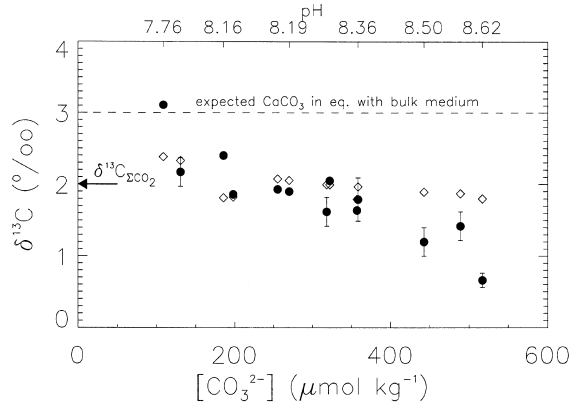

Fig. 11. Model results (open diamonds) and laboratory data (closed circles) in the dark for the $\delta^{13}C$ of the shell as a function of CO_3^{2-} ion concentration and pH (upper horizontal axis). The reported error bars of the laboratory data are in some cases smaller than the diameter of the circles. The model results are in fair agreement within the pH range from 7.7 to 8.4. The larger slope observed in the laboratory data for high CO_3^{2-} concentrations is discussed in Section 4.3.2.

for these two data points in comparison to the mean value (~ 2720 μeq kg^{-1}). The low ΣCO_2 resulting from the low alkalinity explains the calculated low $\delta^{13}C$ of the shell (the amount of isotopically 'light' respired CO_2 is larger relative to the concentration of CO_2 in the bulk medium).

The model $\delta^{13}C$ is in fair agreement with culture data in the pH range from 7.76 to about 8.4 which includes the pH range of the deep and surface ocean between the last glacial maximum and the Holocene period (Sanyal et al., 1995). The slope of the decrease of $\delta^{13}C$ of the calcite with increasing CO_3^{2-} concentration, however, is more pronounced in the laboratory data than in the model calculated values. The very low values of $\delta^{13}C$ above pH 8.4 cannot be satisfactory explained by the model with the standard model setup. The key parameters which influence the model outcome for the slope of $\delta^{13}C$ vs. $[CO_3^{2-}]$ will be discussed in Section 4.3.2.

4.2.3. Comparison with laboratory data (light conditions)

The model was run for the reported pH and sea water alkalinity of the culture experiments of *O. universa* in the light. The calcification and respiration rate was 3.0 and 2.1 nmol h^{-1}, respectively (see Table 1). While there are no data available on the variability of respiration and calcification as a function of the sea water pH, there is evidence that photosynthesis is decreasing with increasing pH. Spero et al. (1991) reported a photosynthetic uptake of 7.2 nmol h^{-1} of *O. universa* at pH 8.15. However, Rink (unpublished data) measured a mean photosynthetic rate of only 2.8 nmol h^{-1} at pH 8.9. Even though, the symbiotic algae utilize CO_2 and presumably additional HCO_3^- (and therefore should not be limited by the availability of CO_2) photosynthesis seems to be reduced at low CO_2 concentrations. This effect might be due to the low carbon dioxide concentration, to physiological stress at high pH values, or both.

Diminished symbiont photosynthesis at high pH was included in the model calculations by a linear relationship between the photosynthetic uptake (F_{phs}) and the bulk CO_2 concentration (see Fig. 12). From the measured values by Rink at pH 8.9 (2.8 nmol h^{-1}) and by Spero et al. (1991) at pH 8.15 (7.2 nmol h^{-1}) the linear relationship was determined. At high CO_2 concentration photosynthesis will reach its maximum value (saturation). The highest value found in the literature (Jørgensen et al., 1985) was therefore chosen for F_{phs} at saturation. The total carbon uptake of 12.44 nmol C h^{-1} for $[CO_2]_{bulk} > 28$ μmol kg^{-1} corresponds to the reported maximum photosynthetic rate of 15 nmol O_2 production h^{-1} (for details about the conversion between oxygen production and carbon uptake, see Wolf-Gladrow et al. (1999)).

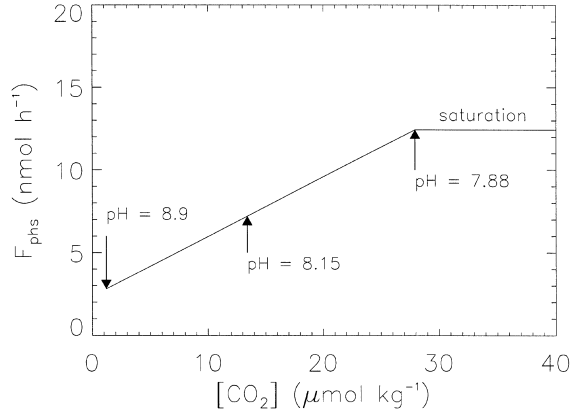

Fig. 12. Photosynthetic uptake (F_{phs}) of the symbiont community as a function of the CO_2 concentration of the bulk medium. A linear relationship between the measured uptake rates for *O. universa* of Rink (unpublished data) at pH 8.9 and of Spero et al. (1991) at pH 8.15 was assumed. The saturation value of 12.44 nmol C h^{-1} at high CO_2 concentration corresponds to the reported maximum photosynthesis of 15 nmol O_2 production h^{-1} measured by Jørgensen et al. (1985) (for details about the conversion between oxygen production and carbon uptake, see Wolf-Gladrow et al. (1999)).

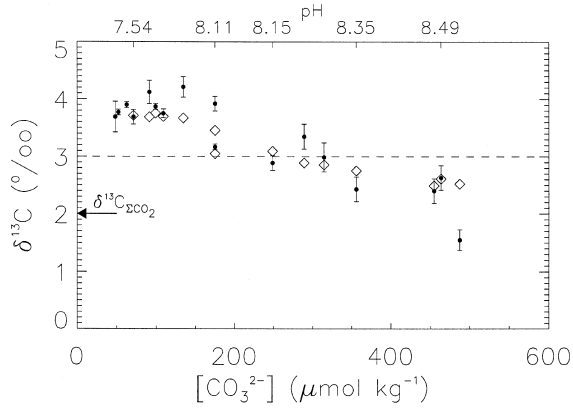

Fig. 13. Model results (open diamonds) and laboratory data (closed circles) in the light for the shell $\delta^{13}C$ of *O. universa* as a function of the carbonate ion concentration. The slightly smaller decrease of the calculated values with increasing $[CO_3^{2-}]$ is again a result of the dark simulation (compare Fig. 11). As in laboratory experiments light conditions in the model refer to a 12:12-h day/night cycle. Thus, the calculated values are influenced by the results of the dark simulation by 50%.

Model results for the $\delta^{13}C$ of the shell under light conditions (open diamonds) and laboratory data obtained for a 12:12-h day/night cycle (filled circles) are presented in Fig. 13. The agreement between model results and measured values is quite satisfactory. The smaller negative slope of modelled shell $\delta^{13}C$ at high carbonate ion concentration is again a result of the dark simulation: Since each diamond represents the arithmetic mean of a dark and light experiment at this carbonate ion concentration, the dark simulation accounts for 50% of the obtained value. At high CO_3^{2-} ion concentration photosynthesis is reduced (see above) and respiration in the dark becomes the dominant process. Thus, at high pH the slope of shell $\delta^{13}C$ vs. $[CO_3^{2-}]$ is determined to a large degree by the results of the dark simulation.

4.3. The response to parameter variations

A number of parameters have been implemented to run the diffusion-reaction model. In this section, it is investigated to what degree the parameterizations and parameter values affect the model outcome.

4.3.1. CO_3^{2-} and HCO_3^- uptake

The model results presented in the preceding sections were obtained under the assumption that CO_3^{2-} is used for calcification. The carbon species which is also likely to be used for calcification is HCO_3^-. The assumption of CO_3^{2-} utilization in *O. universa* is based on results of culture experiments which showed that the shell weight of *O. universa* increases with increasing carbonate ion concentration. If HCO_3^- is the primary source for calcification this effect is difficult to understand. For example, over the pH range 7.5 to 8.5, $[HCO_3^-]$ decreases from ca. 2200 to ca. 1400 μmol kg^{-1}, while $[CO_3^{2-}]$ increases from ca. 65 to ca. 365 μmol kg^{-1}. Thus, if the increase in shell weight in *O. universa* is attributed to the availability of the source, the primary source should be CO_3^{2-}. However, the uptake of HCO_3^- for calcification cannot generally be ruled out. It is possible that *O. universa* partially utilizes HCO_3^-, whereas other species might even use HCO_3^- as the primary source. The influence of HCO_3^- uptake on the model outcome is therefore investigated.

The uptake of CO_3^{2-} is determined by the chemical reaction

$$Ca^{2+} + CO_3^{2-} \rightarrow CaCO_3 \qquad (45)$$

whereas the uptake of HCO_3^- is commonly described by

$$Ca^{2+} + 2\,HCO_3^- \rightarrow CaCO_3 + CO_2 + H_2O. \quad (46)$$

It can be seen from Eq. (46) that the stoichiometry requires that one molecule CO_2 is released for each molecule $CaCO_3$ precipitated, whereas two molecules HCO_3^- are consumed. In the model, the produced CO_2 is released at the surface of the foraminiferal shell and added to the respired CO_2 of the host.

Fig. 14 shows model results of the dark simulation for *O. universa* for CO_3^{2-} uptake (solid lines) and the calculated profiles for HCO_3^- uptake (dashed lines). The input calcification rate is 1 nmol h^{-1}. Thus, for HCO_3^- uptake 2 nmol HCO_3^- h^{-1} are taken up, whereas 1 nmol CO_2 h^{-1} is added to the respiration of the host (2.1 nmol h^{-1}) resulting in a total release of 3.1 nmol CO_2 h^{-1} at the shell (Fig. 14a, dashed line). The HCO_3^- concentration (Fig. 14b) increases towards the shell for both scenarios because respired CO_2 is converted to HCO_3^-. In the case of HCO_3^- uptake, a gradient is established at the shell, reflecting the flux of HCO_3^- towards the shell. It is emphasized that both, respiration and calcification have minor influence on the HCO_3^- profile. Because of the size of the HCO_3^- reservoir ($\sim$ 2170 μmol kg^{-1}) the change is less than 4% with respect to the bulk medium.

The decrease in the CO_3^{2-} concentration towards the shell (Fig. 14c) is slightly more pronounced for CO_3^{2-} uptake (solid line) than for HCO_3^- uptake (dashed line). It is obvious from the CO_2 and pH profile that the CO_2 released at the surface of the shell is the dominant process (the medium close to the shell gets more acid).

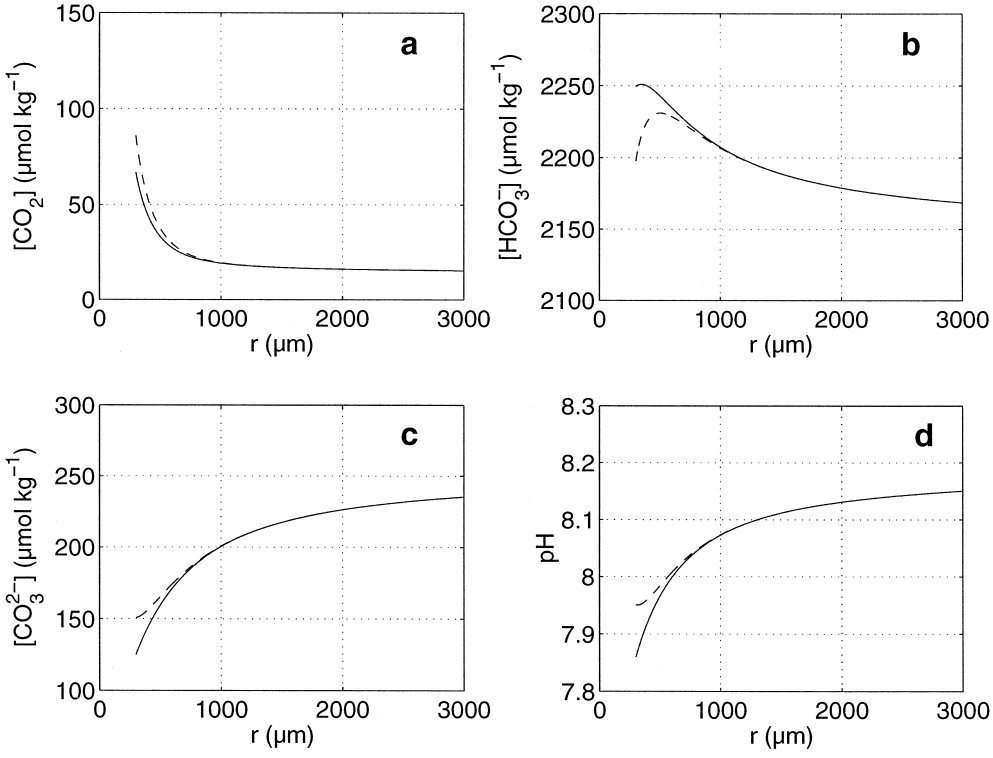

Fig. 14. Model results for the concentration profiles of (a) CO_2, (b) HCO_3^-, (c) CO_3^{2-}, and (d) pH in the dark for different sources of the calcification. Calcite precipitation via $CO_3^{2-} + Ca^{2+} \rightarrow CaCO_3$ (CO_3^{2-} uptake) is indicated by the solid lines, whereas calcite precipitation via $2HCO_3^- + Ca^{2+} \rightarrow CaCO_3 + CO_2 + H_2O$ (HCO_3^- uptake) is indicated by the dashed lines. In the case of HCO_3^- uptake one molecule CO_2 is released for each $CaCO_3$ precipitated explaining the increase of CO_2 at the surface of the shell.

Particularly, in the case of HCO_3^- uptake, the release of additional CO_2 due to the precipitation of $CaCO_3$ has a similar effect on the CO_3^{2-} profile as the direct uptake of CO_3^{2-}. The pH profile closely follows the buffer (CO_3^{2-}) and drops to about 7.85 and 7.95 at the shell for CO_3^{2-} and HCO_3^- uptake, respectively. The calculated pH values for both scenarios are compatible with measurements by pH microelectrodes in the vicinity of *O. universa* (Rink, 1996) (this also holds for *G. sacculifer* (see Jørgensen et al., 1985; Wolf-Gladrow et al., 1999)). Two conclusions can be drawn from these results. Firstly, from a comparison between modelled profiles and microelectrode measurements neither CO_3^{2-} or HCO_3^- can be favored as the primary source for calcification. Secondly, the utilization of CO_3^{2-} or HCO_3^- has a minor influence on the model outcome for the carbon chemistry in the vicinity of *O. universa*. The effect on the stable carbon isotope fractionation is discussed in the next section.

4.3.2. Slope of $\delta^{13}C$ vs. $[CO_3^{2-}]$ for parameter variations

As shown in Fig. 11, the modelled slope of $\delta^{13}C$ vs. $[CO_3^{2-}]$ for the dark simulation in *O. universa* was insufficient to explain the observed trend seen in the experimental results for high CO_3^{2-} concentrations. The slope given by Spero et al. (1997) is $-0.0061‰ \times (\mu mol\ CO_3^{2-}\ kg^{-1})^{-1}$, whereas the calculated mean slope for the standard model run (input parameters, see Table 1) is $-0.0024‰ \times (\mu mol\ kg^{-1})^{-1}$. Thus, the standard parameterization accounts for ca. 40% of the observed trend. Here we investigate which parameters have the potential to affect the slope and how much they have to be changed to reproduce the observed trend. Model runs were carried out to calculate the influence of parameter variations on the slope of $\delta^{13}C$ vs. $[CO_3^{2-}]$ for the dark simulation in *O. universa*. The results are summarized in Table 2. It turns out that the uptake of HCO_3^- instead of CO_3^{2-} has a minor influence on the isotope discrimination. This also holds for the increase of the respiration rate from 2.1 to 4 nmol h^{-1} (independent of CO_3^{2-} concentration), the decrease of the $\delta^{13}C$ of the respired CO_2 from $-21.9‰$ to $-30‰$, and the increase of the chemical rate constant k_{+1} by one order of magnitude.

When the respiration is increased from 1 to 4 nmol h^{-1} over the pH range 7.7 to 8.6 the model reproduces the desired slope of $-0.0061‰ \times (\mu mol\ kg^{-1})^{-1}$. Thus, if an increase in the respiration rate of *O. universa* of this magnitude would be observed with increasing pH, the model results suggest that increased respiration might be the reason for the observed decrease in shell $\delta^{13}C$ vs. $[CO_3^{2-}]$. Unfortunately, changes of the respiration rate in foraminifera with changing pH have not been quantified yet (see discussion).

What is referred to as 'kinetic effect' in Table 2 has a similar impact on the model results. In equilibrium the calcite is enriched in the heavier isotope by about 1‰ with respect to CO_3^{2-} (see, e.g., Fig. 5). Thermodynamic equilibrium implies that a permanent carbonate ion exchange between the calcite lattice and the dissolved species (simultaneous precipitation and dissolution) occurs such that the statistics of this process dictate the isotope discrimination: the heavier isotope is slightly enriched in the calcite. Therefore, equilibrium fractionation demands that the carbonate ions absorbed on the surface of the calcite are exposed for a certain time interval to

Table 2
The influence of parameter variation on $\delta^{13}C$ vs. $[CO_3^{2-}]$

Parameter	Value	Standard	Slope ($‰ \times (\mu mol\ kg^{-1})^{-1}$)
All (Standard)	see Table 1	see Table 1	−0.0024
Uptake	HCO_3^-	CO_3^{2-}	−0.0021
Respiration	4 nmol h^{-1}	2.1 nmol h^{-1}	−0.0033
Respiration[a]	1–4 nmol h^{-1}	constant	−0.0061
$\delta^{13}C$ of respiration	−30‰	−21.9‰	−0.0028
Kinetic effect[b]	yes	no	−0.0061
Rate constant k_{+1}	0.36 s^{-1}	0.036 s^{-1}	−0.0030

[a] The respiration rate was increased from 1 to 4 nmol h^{-1} over the pH range 7.7 to 8.6.
[b] See text.

the calcifying fluid (to guarantee the described exchange) before the ions are buried below subsequently formed layers of the crystal. If calcification proceeds faster at higher carbonate ion concentrations, this process is hindered and the isotopic composition of the calcite will carry the isotopic fingerprint of the source (or is isotopically lighter because the lighter isotope has a smaller activation energy and is kinetically preferred in both directions of the reaction). This process is called kinetic fractionation.

To estimate the possible influence of this mechanism on the model results it was assumed as a first guess that at high CO_3^{2-} concentration the $\delta^{13}C$ of the calcite equals the $\delta^{13}C$ of the source (CO_3^{2-}) at the site of calcification, i.e., the constant offset of ca. 1‰ between CO_3^{2-} and $CaCO_3$ was removed for high $[CO_3^{2-}]$. As a result, the obtained slope for $\delta^{13}C$ vs. $[CO_3^{2-}]$ increased from $-0.0024‰ \times (\mu mol\ kg^{-1})^{-1}$ (standard model run) to $-0.0061‰ \times (\mu mol\ kg^{-1})^{-1}$ (including the kinetic effect). Possible reasons for the nonequilibrium fractionation at the site of calcification are discussed in Section 5.

5. Discussion and conclusions

The results of the numerical model indicate that the enrichment and depletion of ^{13}C in the shell calcite of *O. universa* can be explained in terms of calcite precipitation within an isotopically altered microenvironment. The medium within the vicinity of the foraminifer is strongly perturbed by life processes of the host–symbiont system and therefore differs significantly from the bulk medium with regard to the concentrations and the isotopic compositions of the carbonate species. The calculated $\delta^{13}C$ of the shell is lowered by 'light' respired CO_2, while it is enriched in ^{13}C through photosynthesis. The calculated difference between dark and light conditions ($\sim 1.5‰$) are consistent with laboratory measurements (see Fig. 7). Within the uncertainties of the biological input parameters, the model adequately describes the increase of shell $\delta^{13}C$ vs. light intensity at low light as well as the saturation values at high light. In addition, model calculations predicted limited calcification rates at low pH in the dark (Section 4.2.1, Fig. 9c) which are confirmed by observed incomplete calcification or dissolution of the calcite at pH values of 7.3.

It should be pointed out that despite the somewhat lengthy mathematical formalism, the concept of the model is straightforward and is based on the inorganic carbonate chemistry (no elaborate enzyme kinetics is required). Since the basic features of carbon isotope fractionation in foraminifera can be reproduced, we believe that the model includes the essential mechanisms which determine the isotope discrimination during calcite precipitation. However, some questions remain unaddressed.

There is evidence that certain foraminifera accumulate carbon and calcium within an internal pool and utilize it when new chambers are added (this calcite precipitation often occurs within a very short time interval). The possible carbon isotope fractionation associated with the accumulation into or the release from this internal pool is unknown but might influence the $\delta^{13}C$ of the shell calcite to a large degree. Spero et al. (1977) demonstrated that the decrease in $\delta^{13}C$ of the shell with increasing CO_3^{2-} ion concentration (carbonate ion effect) is much more pronounced in the symbiont barren species *G. bulloides* which adds chambers intermittently and is therefore likely to have an internal pool (see Wolf-Gladrow et al., 1999). *Orbulina universa*, however, calcifies the terminal spherical chamber continuously within 5–7 days and does not rely on an internal pool because the calcium and carbon demand during calcification can be met by diffusion from the surrounding seawater alone. Thus, the different slopes of $\delta^{13}C$ vs. carbonate ion concentration for these two species might be attributed to different calcite precipitation mechanisms.

Even though, the model assumptions seem to work satisfactory for *O. universa*, discrepancies between the model outcome and observed data are present and should be further investigated. The trend of decreasing $\delta^{13}C$ of the shell with increasing CO_3^{2-} ion concentration was reproduced by the model and is attributed to an increasing incorporation of 'light' respired CO_2 at higher pH into the shell (see Fig. 11). The larger negative slope of the culture data in comparison to the model outcome, however, was not reproduced. From Table 2 it is

obvious that the observed slope could be explained by the model if the respiration rate of the foraminifer increases systematically with higher carbonate ion concentration. The CO_2 concentration of the bulk medium is very small at high pH (ca. 2 μmol kg^{-1} at pH 8.8). If the CO_2 release of the foraminifer is a function of the CO_2 gradient between the external and internal carbon dioxide concentration ($[CO_2]$ of bulk medium and inside the cell), one could argue that the stronger gradient at high pH increases the CO_2 efflux at higher carbonate ion concentration. However, this argument is speculative since there are no data available on the CO_2 efflux from foraminiferal cells at different pH values.

Another mechanism to explain the missing coherence in the modelled and observed slope might be an increasing kinetic fractionation (depletion of ^{13}C) in the calcite with increasing precipitation rate at higher carbonate ion concentration. Romanek et al. (1992) found no dependence of the $\delta^{13}C$ of inorganically formed calcite on the precipitation rate. However, Turner (1982) reported a depletion of ^{13}C in calcite with increasing precipitation rate. In general, the product of a chemical reaction (kinetic process in one direction) is depleted in the heavier isotope. From the fact that $CaCO_3$ at normal sea water pH is enriched in the heavier isotope relative to the source (CO_3^{2-} or HCO_3^-), it follows that the ratio of precipitation to dissolution (ratio of reactions in forward and backward direction) must be closer to equilibrium at normal pH. Consequently, one would expect a 'heavy' calcite for small precipitation rates and 'light' calcite for high precipitation rates. If the precipitation rate goes to infinity, the $\delta^{13}C$ of the calcite should be equal to or smaller than that of the carbon source. Hence, the larger negative slope of the observed shell $\delta^{13}C$ vs. $[CO_3^{2-}]$ could be due to a kinetic fractionation effect through increased precipitation rates at high pH (Table 2). These questions should be clarified by experimental investigations which are currently in preparation by members of our group.

Despite the discrepancies between model results and observations it should be emphasized that the fact that the shell $\delta^{13}C$ of foraminifera decreases with increasing carbonate ion concentration is observed in laboratory measurements and is predicted by the model. An increase of $[CO_3^{2-}]$ from 248 to 355 μmol kg^{-1} (equivalent to an 0.2 units increase in pH from 8.15 to 8.35, see Fig. 13) produced a decrease of 0.35‰ in the modelled shell $\delta^{13}C$. This fact may have important consequences for the interpretation of paleoceanographical data. For instance, it was proposed by Shackleton (1977) that the decrease in the $\delta^{13}C$ of foraminiferal calcite (direct proxy for $\delta^{13}C_{\Sigma CO_2}$) during the last glacial maximum was brought about by the transfer of isotopically light carbon from the terrestrial biosphere to the atmosphere–ocean system. However, part of the effect of decreasing $\delta^{13}C$ during the last glaciation might be attributed to changes in ocean chemistry (Sanyal et al., 1995; Lea et al., in press).

The relevance of our results to paleoceanographic studies seems limited by the fact that *O. universa* is not widely used for reconstructions. *Orbulina universa* is a spinose, symbiont bearing species, whereas other commonly used species for proxy studies are symbiont barren or non-spinose. However, the basic mechanisms which control stable carbon isotope fractionation in *O. universa* should be applicable to other foraminifera as well. This statement is based on the observation that the general effect of the carbonate ion concentration on the $\delta^{13}C$ of foraminiferal calcite appears to be independent of the species chosen (whether symbiont bearing or symbiont barren), even though the magnitude of the effect is species-dependent. The carbonate ion effect was hitherto demonstrated in the symbiont bearing species *O. universa*, *G. sacculifer*, and *G. ruber*, and in the symbiont barren species *G. bulloides* (Spero et al., 1997; Bijma et al., unpublished data). The magnitude of the trend, however, varies for different species and might be attributed to different calcification mechanisms (e.g., calcification via an internal pool).

The results of the dark simulation for *O. universa* should be comparable to a symbiont barren species, provided that the geometry of the shell, the dark respiration of the symbionts, and physiological differences have a minor influence. For non-spinose species such as *Neogloboquadrina dutertrei* culture experiments are desired to investigate the response of isotope discrimination to sea water changes.

We conclude that more detailed work is needed on the carbonate ion effect in other species and on the underlying mechanisms such as the interaction between sea water chemistry and vital effects which determine the isotopic composition of the shells. This will hopefully lead to a sound understanding of carbon (but also of

oxygen and boron) isotope fractionation in foraminifera (Zeebe, in press) and a better interpretation of paleoceanographical data in the future.

Acknowledgements

We would like to thank Marion O'Leary for discussions about fractionation in chemical reactions. Suggestions by Howard J. Spero and Abhijit Sanyal are gratefully acknowledged. The comments of two anonymous referees were of great value and have improved the manuscript. Alfred-Wegener-Institut für Polar- und Meeresforschung publication 1504.

References

Bé, A.W.H., 1977. An ecological, zoogeographic and taxonomic review of recent planktonic foraminifera. In: Ramsay, A.T.S. (Ed.), Oceanic Micropaleontology, Vol. 1, London, pp. 1–100.

Bijma, J., Spero, H.J., Lea D.W., Archer, D., in press. Reassessing foraminiferal stable isotopes: Effects of seawater carbonate chemistry. In: Fischer, G., Wefer, G. (Eds.), Proxies in Paleoceanography, Springer.

Boudreau, B.P., Canfield, D.E., 1993. A comparison of closed- and open-system models for porewater pH and calcite-saturation state. Geochim. Cosmochim. Acta 57, 317–334.

Cussler, E.L., 1984. Diffusion. Mass transfer in fluid systems, Cambridge Univ. Press, New York, pp. 105–124.

Descolas-Gros, C., Fontugne, M.R., 1985. Carbon fixation in marine phytoplankton: carboxylase activities and stable carbon-isotope ratios; physiological and paleoclimatological aspects. Mar. Biol. 87, 1–6.

DOE, 1994. Dickson, A.G., Goyet, C. (Eds.), Handbook of Methods for the Analysis of the Various Parameters of the Carbon Dioxide System in Sea Water, Version 2, ORNL/CDIAC-74.

Falkowski, P.G., 1991. Species variability in the fractionation of ^{13}C and ^{12}C by marine phytoplankton. J. Plankton Res. 13, 21–28, Suppl.

Francois, R., Altabet, M.A., Goericke, R., McCorkle, D.C., Brunet, C., Poisson, A., 1993. Changes in the $\delta^{13}C$ of surface water particulate organic matter across the subtropical convergence in the S. W. Indian Ocean. Glob. Biogeochem. Cycles 7, 627–644.

Goericke, R., Fry, B., 1994. Variations of marine plankton $\delta^{13}C$ with latitude, temperature and dissolved CO_2 in the world ocean. Glob. Biogeochem. Cycles 8, 85–90.

Hemleben, Ch., Spindler, M., Anderson, O.R., 1989. Modern Planktonic Foraminifera, Springer Verlag, New York.

Jähne, B., Heinz, G., Dietrich, W., 1987. Measurement of the diffusion coefficients of sparingly soluble gases in water. J. Geophys. Res. 92, 10767–10776.

Jassby, A.D., Platt, T., 1976. Mathematical formulation of the relationship between photosynthesis and light for phytoplankton. Limnol. Oceanogr. 21 (4), 540–547.

Jørgensen, B.B., Erez, J., Revsbech, N.P., Cohen, Y., 1985. Symbiotic photosynthesis in a planktonic foraminiferan, *Globigerinoides sacculifer* (Brady), studied with microelectrodes. Limnol. Oceanogr. 30 (6), 1253–1267.

Lea, D.W., Martin, P.A., Chan, D.A., Spero, H.J., 1995. Calcium uptake and calcification rate in the planktonic foraminifer *Orbulina universa*. J. Foram. Res. 25, 14–23.

Lea, D.W., Bijma, J., Spero, H.J., Archer, D., in press. Implications of a carbonate ion effect on shell carbon and oxygen isotopes for glacial ocean conditions. In: Fischer, G., Wefer, G. (Eds.), Proxies in Paleoceanography, Springer.

Li, Y.H., Gregory, S., 1974. Diffusion of ions in sea water and in deep-sea sediments. Geochim. Cosmochim. Acta 38, 703–714.

Mackin, J.E., 1986. The free-solution diffusion coefficient of Boron: influence of dissolved organic matter. Mar. Chem. 20, 131–140.

Mook, W.G., 1986. ^{13}C in atmospheric CO_2. Netherlands Journal of Sea Research 20 (2/3), 211–223.

O'Leary, M.H., 1981. Carbon isotope fractionation in plants. Phytochemistry 20, 553–557.

O'Leary, M.H., 1984. Measurement of the isotope fractionation associated with diffusion of carbon dioxide in aqueous solution. J. Phys. Chem. 88, 823–825.

O'Leary, M.H., Madhavan, S., Paneth, P., 1992. Physical and chemical basis of carbon isotope fractionation in plants. Plant, Cell and Environment 15, 1099–1104.

Rau, G.H., Takahashi, T., Des Marais, D.J., Repeta, D.J., Martin, J.H., 1992. The relationship between $\delta^{13}C$ of organic matter and $[CO_2(aq)]$ in ocean surface water: Data from a JGOFS site in the northeast Atlantic Ocean and a model. Geochim. Cosmochim. Acta 56, 1413–1419.

Rau, G.H., Riebesell, U., Wolf-Gladrow, D., 1996. A model of photosynthetic ^{13}C fractionation by marine phytoplankton based on diffusive molecular CO_2 uptake. Mar. Ecol. Prog. Ser. 133, 275–285.

Rink, S., 1996. Untersuchung der Photosynthese und Respiration der symbiontentragenden planktischen Foraminifere *Orbulina universa*, Universität Bremen.

Rink, S., Kühl, M., Bijma, J., Spero, H.J., 1998. Microsensor studies of photosynthesis and respiration in the symbiotic foraminifer *Orbulina universa*. Mar. Biol. 131, 583–595.

Romanek, Ch.S., Grossman, E.L., Morse, J.W., 1992. Carbon isotopic fractionation in synthetic aragonite and calcite: effects of temperature and precipitation rate. Geochim. Cosmochim. Acta 56, 419–430.

Sanyal, A., Hemming, N.G., Hanson, G.N., Broecker, W.S., 1995. Evidence for a higher pH in the glacial ocean from boron isotopes in foraminifera. Nature 373, 234–236.

Sanyal, A., Hemming, N.G., Broecker, W.S., Lea, D.W., Spero, H.J., Hanson, G.N., 1996. Oceanic pH control on the boron isotopic composition of foraminifera: evidence from culture experiments. Paleoceanography 11, 513–517.

Shackleton, N.J., 1977. in The fate of fossil fuel CO_2. In: Anderson, N.R., Malahoff, A. (Eds.), The Oceans, Plenum, New York, pp. 401–427.

Shackleton, N.J., Hall, M.A., Line, J., Shuxi, C., 1983. Carbon isotope data in core V19-30 confirm reduced carbon dioxide concentration in the ice age atmosphere. Nature 306, 319–322.

Spero, H.J., 1992. Do planktic foraminifera accurately record shifts in the carbon isotopic composition of sea water ΣCO_2?. Mar. Micropaleontol. 19, 275–285.

Spero, H.J., DeNiro, M.J., 1987. The influence of symbiont photosynthesis on the $\delta^{18}O$ and $\delta^{13}C$ values of planktonic foraminiferal shell calcite. Symbiosis 4, 213–228.

Spero, H.J., Williams, D.F., 1988. Extracting environmental information from planktonic foraminiferal $\delta^{13}C$ data. Nature 335, 717–719.

Spero, H.J., Lea, D.W., 1996. Experimental determination of stable isotope variability in Globigerina bulloides: implications for paleoceanographic reconstructions. Mar. Micropaleontol. 28, 231–246.

Spero, H.J., Lerche, I., Williams, D.F., 1991. Opening the carbon isotope 'vital effect' black box: 2. Quantitative model for interpreting foraminiferal carbon isotope data. Paleoceanography 6, 639–655.

Spero, H.J., Bijma, J., Lea, D.W., Bemis, B.E., 1997. Effect of seawater carbonate concentration on foraminiferal carbon and oxygen isotopes. Nature 390, 497–500.

Turner, J.V., 1982. Kinetic fractionation of carbon-13 during calcium carbonate precipitation. Geochim. Cosmochim. Acta 46, 1183–1191.

Wefer, G., Berger, W.H., 1991. Isotope paleontology: growth and composition of extant calcareous species. Mar. Geol. 100, 207–248.

Wolf-Gladrow, D.A., Riebesell, U., 1997. Diffusion and reactions in the vicinity of plankton: a refined model for inorganic carbon transport. Mar. Chem. 59, 17–34.

Wolf-Gladrow, D.A., Bijma, J., Zeebe, R.E., 1999. Model simulation of the carbonate system in the microenvironment of symbiont bearing foraminifera. Mar. Chem. 64, 181–198.

Wong, W.W., Sackett, W.M., 1978. Fractionation of stable carbon isotopes by marine phytoplankton. Geochim. Cosmochim. Acta 42, 1809–1815.

Zeebe, R.E., in press. An explanation of the effect of sea water carbonate concentration on foraminiferal oxygen isotopes. Geochim. Cosmochim. Acta.